이학박사학위논문

생쥐의 사지발생 과정에서
SWI/SNF 염색사 리모델링 복합체의 기능에 관한 연구

Studies on the function of SWI/SNF chromatin remodeling complex during limb development

2015 년 7 월

서울대학교 대학원

생명과학부

전 신

생쥐의 사지발생 과정에서
SWI/SNF 염색사 리모델링 복합체의 기능에 관한 연구

Studies on the function of SWI/SNF chromatin remodeling complex during limb development

지도교수 성 노 현

이 논문을 이학박사학위논문으로 제출함

2015 년 7 월

서울대학교 대학원

생명과학부

전 신

전신의 박사학위논문을 인준함

2015 년 7 월

위 원 장 _____ (인)

부위원장 _____ (인)

위 원 _____ (인)

위 원 _____ (인)

위 원 _____ (인)

ABSTRACT

During development and differentiation, alterations in gene expression require modification of chromatin status, which allows or restrains the access of transcription factors to the regulatory elements. For developmental progression, the function of context-dependent transcription factors responding to developmental signals needs the recruitment of chromatin remodelers. Recent studies have identified the interlinked transcriptional networks by the enrichment of these factors in the genomic loci by using a limb bud, which is an excellent model to understand tissue patterning. Thus, the molecular circuits of regulators orchestrating limb development involve distinct functions of chromatin remodelers. The graded Sonic hedgehog (Shh) signaling governs the vertebrate limb skeletal patterning along anteroposterior (AP) axis by regulating the activity of bifunctional Gli transcriptional regulators acting as activator or repressor. Gli target genes are activated, repressed or derepressed in response to a gradient of Hedgehog (Hh) signaling, but the mechanisms by which bifunctional Gli proteins collaborate to regulate target genes are poorly understood. Furthermore, the genetic networks involved in limb patterning are well defined, whereas the epigenetic control of the process by chromatin remodelers remains unclear.

Here, I found that *Srg3*/*mBaf155*, a core subunit of SWI/SNF chromatin remodeling complex, is essential for Shh/Gli-driven limb AP skeletal patterning. Genetic analysis and spatiotemporal distributions of gene expression analyzed by whole-mount *in situ* hybridization have uncovered the dual requirements of SWI/SNF complex in Hh pathway during limb development. Specific inactivation of *Srg3* in the limb bud mesenchyme hampered the transcriptional upregulation of both Shh receptor

Ptch1 and its downstream effector *Gli1* upon morphogen Shh stimulation and induced ectopic activation of Hh pathway in Shh-free region. In limb buds lacking *Srg3*, the attenuated sensing of Shh caused the redistribution of *Shh*-descendants as well as the downregulation of target genes. Without severe defects in the formation of signaling centers such as the zone of polarizing activity (ZPA) and the apical ectodermal ridge (AER), *Srg3*-deficient limb buds established the intact AP axis but progressively lost their anterior and posterior identities. Analysis of these progressive phenotypes provided genetic evidence how modulation of Shh responsiveness drives the fate of posterior limb skeletal progenitors and activation of ectopic Hh pathway is detrimental to the formation of anterior skeletal elements. Bifurcating role of Srg3 in Hh pathway distalized the distributions of epithelial-mesenchymal signaling components such as Shh, BMP antagonist Gremlin1 (Grem1) and FGF. Subsequently, *Srg3* deficiency led to aberrant BMP activity and disruption of chondrogenic differentiation in zeugopod and autopod primordia. Notably, I found that Shh responsiveness and Gli repressor activity are collaboratively required for the spatiotemporal regulation of *Grem1* expression, which affects the onset of digit chondrogenesis. My study uncovers the bifurcating function of SWI/SNF complex in Hh pathway to determine the fate of AP skeletal progenitors.

Keywords: SWI/SNF, Srg3, limb patterning, Hh pathway, Grem1

Student number: 2007-30094

TABLE OF CONTENTS

LIST OF FIGURES

LIST OF TABLES

LIST OF ABBREVIATIONS

AER	Apical Ectodermal Ridge
Alx4	Aristaless-like 4
AP	Anteroposterior
BBBA	Benzyl Benzoate/Benzyl Alcohol
BMP	Bone Morphogenetic Protein
BAF	Brg1/Brm-associated factor
Brg1	Brahma related gene 1
BSA	Bovine serum albumin
ChIP	Chromatin immunoprecipitation
CRM	*cis*-regulatory module
DIG	Digoxigenin
FGF	fibroblast growth factor
GliA	Gli activators
GliR	Gli repressors
Grem1	Gremlin1
Hand2	Heart, autonomic nervous system, and other neural crest-derived tissues 2
Hh	Hedgehog
Hox	homeobox gene
Irx	Iroquois homeobox gene
LRM	limb *cis*-regulatory module
MEF	Mouse embryonic fibroblast
Msx	Muscle segment homeobox homolog
Pax9	Paired-box-containing gene

PBST	0.1% Tween-20 in PBS
PD	Proximodistal
PFA	Paraformaldehyde
Ptch1	Patched1
Shh	Sonic Hedgehog
Sox9	SRY-box 9
Srg3	Swi3-related gene
SWI/SNF	switch/sucrose-nonfermentable
ZPA	Zone of Polarizing Activity
ZRS	ZPA regulatory sequence

I. Introduction

I-1. SWI/SNF chromatin remodeling complex

In eukaryotic organisms, DNA is highly packaged into chromatin structure imposed by the nucleosome, which prevents all transcriptional programs (Li et al., 2007). Thus, the activation of transcription requires the structural modulation of chromatin status which permits the access of transcription factors to regulatory elements such as promoters and enhancers of target genes (Narlikar et al., 2002). This plasticity of chromatin accessibility can be ensured by covalently modifying the histone tails of nucleosomes or by moving nucleosome positions and breaking DNA-histone contacts through ATP hydrolysis (Hargreaves and Crabtree, 2011; Kouzarides, 2007; Li et al., 2007). Histone-modifying complexes include enzymes that acetylate, methylate, phosphorylate, SUMOylate and ubiquitylate histones and thereby modified histone residues can be reversed by counteracting enzymes (Kouzarides, 2007). ATP-dependent chromatin remodeling complexes are divided into four groups based on the ATPase subunits, SWI/SNF, ISWI, CHD/NURD/Mi2 and INO80 families (Hargreaves and Crabtree, 2011). Although chromatin-modifying complexes are not sufficient for regulating gene expression, these are indispensable for proper regulation of transcription with context-dependent transcriptional regulators and general transcription machinery.

Among ATP-dependent chromatin remodeling complexes, SWI/SNF complexes are comprised of multi-subunits and evolutionarily conserved among eukaryotes from yeast to vertebrates. The SWI/SNF complex contains a catalytic ATPase subunit with bromodomain recognizing acetylated histones (Hassan et al., 2002), Swi2/Snf2 and Sth2 in yeast (*Saccharomyces cerevisiae*), Brahma (Brm) in fly (*Drosophila melanogaster*), and mutually exclusive Brm and Brahma-related gene 1 (Brg1) in mammal (Khavari et al., 1993; Laurent et al., 1993; Muchardt and Yaniv, 1993;

Tamkun et al., 1992). SWI/SNF subunits including Swi1/Adr6, Swi3, Snf5, and Snf6 were identified from the genetic screens of yeast and these subunits physically associate and coordinately function with Swi2/Snf2 to regulate the transcription (Cairns et al., 1994; Laurent et al., 1991; Laurent and Carlson, 1992; Smith et al., 2003). In fly, the core components of the SWI/SNF complex consist of Osa, Mor, and Snr1, which were identified as trithorax group genes antagonizing the function of polycomb group (PcG) protein, and modulate the function of Brm complexes (Collins et al., 1999; Dingwall et al., 1995; Papoulas et al., 1998; Tamkun et al., 1992). Mammalian SWI/SNF complexes are polymorphic as shown in the combinatorial diversity of BAF (Brg1/Brm-associated factor) complexes selectively assembled by each of BAF250a/b, BAF155/BAF170, BAF60a/b/c, BAF45a/b/c/d, BAF57, BAF53a/b, and BAF47 (Ho et al., 2009b; Lessard et al., 2007; Wang et al., 1996; Wu et al., 2007).

Nucleosome remodeling activity of mammalian SWI/SNF complexes can be increased by the addition of BAF47, BAF155 and BAF170 to BRG1 (Phelan et al., 1999). Furthermore, BAF155/Srg3 (Swi3-related gene) and BAF170 physically interact with core subunits through the conserved domains such as SANT domain, SWIRM domain and leucine-zipper motif and control the stability of SWI/SNF complexes by protecting them from proteasomal degradation (Chen and Archer, 2005; Jung et al., 2012; Sohn et al., 2007). Interaction of specific BAF subunit with transcription factors recruits the SWI/SNF complex to the regulatory region of target genes and involves the cooperative function between the complex and other chromatin modifying complexes (Belandia et al., 2002; Cheng et al., 1999; Harikrishnan et al., 2005; Oh et al., 2008; Zhan et al., 2011).

I-2. The roles of SWI/SNF complex during embryonic development

Constitutive inactivation of *Brg1*, *BAF155*/*Srg3* (hereafter referred as *Srg3*), or *BAF47*/*Snf5* in mice resulted in embryonic lethality during peri-implantation stage, indicating that SWI/SNF complex is essential for early mammalian development (**Figure 1A**) (Bultman et al., 2000; Guidi et al., 2001; Kim et al., 2001; Klochendler-Yeivin et al., 2000). *In vitro* outgrowth analysis showed that $Brg1^{-/-}$ blastocysts failed to hatch, whereas $Srg3^{-/-}$ blastocysts resulted in a developmental arrest after hatching (Bultman et al., 2000; Kim et al., 2001). This requirement of SWI/SNF complex for maintenance and pluripotency of embryonic stem cells (ES cells) has been revealed by the recent proteomic and ChIP-Seq analysis. esBAF complexes, which are purified from ES cells, are defined by the presence of Brg1, Srg3, and BAF60a, and the exclusion of Brm, BAF170, and BAF60c (Ho et al., 2009b). In ES cells, esBAF complexes cooperatively function with core transcription factors Oc4, Sox2 and Nanog, which regulate self-renewal ability and/or pluripotency (Ho et al., 2009a).

Differentiation of neural stem/progenitor cells, which have the capacity to self-renew, into specific neural cell lineages requires the change in epigenetic environments (Borrelli et al., 2008; Hirabayashi and Gotoh, 2010). About twenty percentages of *Brg1* or *Srg3* heterozygotes exhibited exencephaly, suggesting that SWI/SNF complexes play key roles in neural development (**Figure 1B**) (Bultman et al., 2000; Kim et al., 2001). Genetic analysis of *Brg1* in neural stem/progenitor cells showed that Brg1 is required for the maintenance of stem/progenitor cell population in neural development (Lessard et al., 2007). Additionally, Brg1-containing complexes regulate the transcription of components in Notch and Sonic hedgehog

Figure 1. Functions of Srg3-containing SWI/SNF chromatin remodeling complex in mammalian development

(**A**) Brg1 and Srg3 are essential for early embryogenesis. Genetic ablation of *Brg1* or *Srg3* leads to embryonic lethality at the peri-implantation stage.

(**B**) The minority of heterozygous mutants in *Brg1* or *Srg3* exhibits exencephaly.

(**C**) Rescued embryos by Srg3 transgene in homozygous *Srg3* mutants overcome early embryonic lethality but exhibit defects in blood vessel formation and fetal circulation in the yolk sac.

Peri-implantation development

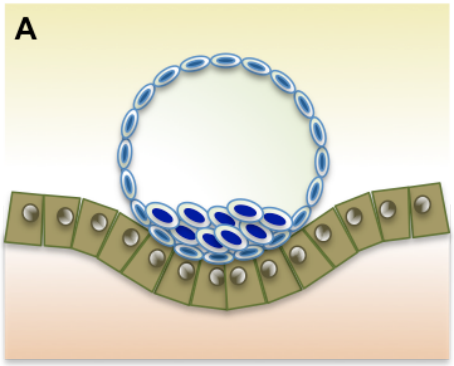

Kim et al. (2001)

Neural development

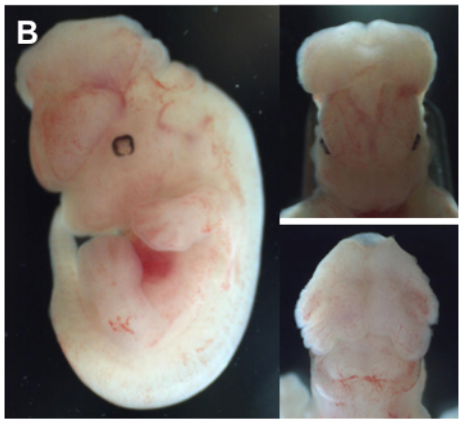

Kim et al. (2001)

Vascular development

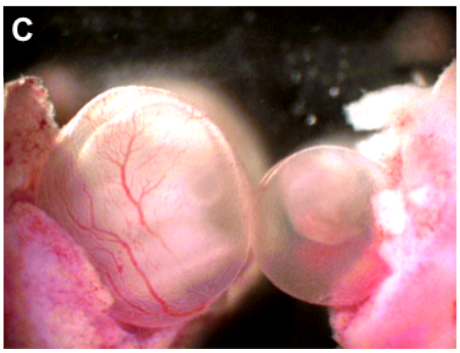

Han et al. (2008)

(Shh) signaling pathways involved in neural development (Lessard et al., 2007; Zhan et al., 2011). Proteomic studies revealed that the switch in BAF subunit composition such as BAF53a to 53b and BAF 45a to -45b/c is essential for neuronal differentiation from proliferating neural progenitors to committed post-mitotic neurons (Lessard et al., 2007; Wu et al., 2007). These studies provide evidence that SWI/SNF complexes function in epigenetic promoting or silencing programs of genes implicated in proliferating neurogenesis and neuronal differentiation.

Analyses of conditional loss-of-function *BAF* subunits in mice have also uncovered the essential requirements of SWI/SNF complex in mammalian development such as heart, muscle, and immune systems including blood vessel formation (**Figure 1C**) (Chi et al., 2002; Choi et al., 2012; Han et al., 2008; Ho and Crabtree, 2010; Lange et al., 2008; Lickert et al., 2004; Takeuchi and Bruneau, 2009; Wang et al., 2004). SWI/SNF complexes contribute to the regulation of multiple target genes at different developmental stages as well as in distinct cell lineages. Furthermore, the interaction of individual BAF subunits with context-dependent transcription factors provides specificity and stability to the epigenetic regulation at the chromatin level.

I-3. Vertebrate limb development

The limb bud is an excellent model to understand the pattern formation in vertebrates and its underlying molecular mechanisms (Zeller et al., 2009). Vertebrate limb development is tightly controlled by epithelial-mesenchymal interactions of two morpho-regulatory signaling centers, the zone of polarizing activity (ZPA) and the

apical ectodermal ridge (AER). Sonic hedgehog (Shh) signaling from the ZPA located in the posterior margin and fibroblast growth factor (FGF) signaling from the AER enclosing the mesenchyme at the distal tip of the limb bud coordinately control anteroposterior (AP) and proximodistal (PD) limb bud patterning (**Figure 2**) (Crossley and Martin, 1995; Riddle et al., 1993; Sun et al., 2002; Zeller et al., 2009).

I-3-1. Function of Shh signal and its regulation in developing limb bud

Hedgehog (Hh) was first identified by genetic screens in *Drosophila* (Nusslein-Volhard and Wieschaus, 1980). Its general principles acting as a secreted protein and evolutionarily conserved roles of three vertebrate counterparts, Shh, Indian hedgehog (Ihh) and desert hedgehog (Dhh) were revealed during organogenesis (Ingham and McMahon, 2001). In particular, Shh activity can reproduce the action of notochord and floor plate in the neural tube and of ZPA in the limb bud (Jessell, 2000; Riddle et al., 1993).

Cell fate marking studies in mouse limb have revealed that Shh signaling regulates identities of limb skeletal elements such as ulna and digits 2 to 5 depending on the concentration and exposed time to its signal (Ahn and Joyner, 2004; Harfe et al., 2004; Scherz et al., 2007). As the descendants of *Shh*-expressing cells expand anteriorly away from the ZPA, the temporal and spatial gradients of morphogen Shh and its responsiveness specify digits 2 to 5 (**Figure 3**). Thus, limbs lacking *Shh* result in the loss of posterior skeletal elements that develops one anterior zeugopod bone and the anterior-most single digit (Chiang et al., 2001). In addition, Shh signal patterns digit identity only at very early and transient phase after its expression is activated (about 12 hr), and thereafter continuously regulates the expansion of digit progenitors (Zhu et al., 2008). While previous studies have demonstrated that the formation of limb

skeletal structures such as radius and thumb in Shh-free anterior region is independent on Shh signaling, recent works suggested that Shh inhibits their formation (Li et al., 2014a; Xu et al., 2013). However, the mechanisms underlying the inhibitory roles of Shh in the anterior skeletal formation are unclear.

The initiation and spatial restriction of *Shh* expression within the ZPA is controlled by a far upstream cis-regulatory module (CRM), which is known as the limb-specific enhancer ZPA regulatory sequence (ZRS) (Anderson et al., 2014; Lettice et al., 2003). In the limb bud, the interaction of transcriptional regulators ETS, HAND2, HOX, PBX, and TBX3 with the ZRS defines and activates the localized expression of *Shh* (Capellini et al., 2006; Galli et al., 2010; Lettice et al., 2012; Osterwalder et al., 2014; Tarchini et al., 2006). By contrast, loss-of-function mutants in ETV, GATA6, and TWIST1 exhibit anterior ectopic *Shh* expression, resulting in preaxial polydactyly (a type of polydactyly with additional digits in the anterior autopod) (Kozhemyakina et al., 2014; Mao et al., 2009; Zhang et al., 2009; Zhang et al., 2010). These regulators differentially occupy distinct sites or competitively bind to the same sites of ZRS. Unlike ZRS-mediated transactivation, genetic ablation of several factors such as GLI3 and ALX4 also induces ectopic *Shh* expression in the anterior mesenchyme (Buscher et al., 1997; Qu et al., 1998), but the mechanisms that can repress Shh are unknown.

I-3-2. The Hedgehog signaling pathway and function of GLI proteins

In vertebrates, binding of Shh ligand to its receptor Patched1 (Ptch1) enables the signal transduction through derepression of signal transducer Smoothened, allowing Gli family transcription factors (Gli1, Gli2, and Gli3) to function as activators (Hui and Angers, 2011). The transcriptional upregulation of *Ptch1*, serving as a sensitive readout of Shh activity, is required for sequestering diffusible ligands to restrain their

spread within the target range (Briscoe et al., 2001; Chen and Struhl, 1996). Notably, the spatiotemporal regulation of *Ptch1* expression is important to prevent aberrant activation of Hedgehog (Hh) signaling, indicating that Ptch1 functions as the negative regulator of Hh signaling (Butterfield et al., 2009; Zhulyn et al., 2014). Interestingly, a recent report showed that evolutionary alterations of *Ptch1* CRM restrict the response to graded Shh signaling, causing loss of digit asymmetry in bovine autopods (Lopez-Rios et al., 2014).

Zinc-finger proteins of Gli family, which are also known as Cubitus interruptus (Ci) in *Drosophila melanogaster*, act as transcriptional activators (GliA) or repressors (GliR) of Hh signaling (Briscoe and Therond, 2013). Gli proteins recognize and bind to a consensus sequence GACCACCCA within the regulatory loci of target genes through the DNA-binding domain including zinc-finger motifs (Kinzler et al., 1988; Kinzler and Vogelstein, 1990; Orenic et al., 1990). Genome-scale analyses by chromatin immunoprecipitation (ChIP) and gene expression profiling have revealed a number of putative Gli target genes in limb and neural development and tumorigenesis (Lee et al., 2010; Vokes et al., 2007; Vokes et al., 2008). Gli transcriptional targets are categorized into two groups: for transcription progression, Gli activator genes that require GliA and Gli derepression genes that are induced in the absence of GliR (Li et al., 2014b). Gli activator genes mainly drive threshold responses to graded Hh signaling by competition between GliA and GliR (Jacob and Briscoe, 2003; Wang et al., 2000), whereas the mechanism by which Gli derepression genes are repressed remains unclear.

The full-length activators Gli2A and Gli3A in cells responding to Shh contribute to the activation of Shh target genes including transcription of *Gli1*, which might act as an indicator of Shh signaling range in limb development (Bai et al., 2004; Dai et al.,

1999; Park et al., 2000). The absence of Shh signaling allows for the proteolytic processing of bifunctional Gli2 and Gli3 to truncated repressors Gli2R and Gli3R (GliR) (Pan et al., 2006; Wang et al., 2000). Thus, the graded Shh-mediated processing generates gradients such as high GliA in the posterior and predominant Gli3R in the anterior (**Figure 3**).

While *Gli1* and *Gli2* are not essential for limb development (Park et al., 2000), mutants constitutively lacking *Gli3* exhibited preaxial and central polydactylies fused with soft tissues (polysyndactyly) (Hui and Joyner, 1993). Gli3 functions as a major regulator of AP digit patterning and Gli2 has compensatory roles of Gli3 activity (Ahn and Joyner, 2004; Bowers et al., 2012; Litingtung et al., 2002; te Welscher et al., 2002b). During early limb bud development, prior to the onset of ZPA-*Shh* expression, *Gli3* is required for establishing AP polarity through genetic antagonism with *Hand2* and is involved in the formation of two signaling centers ZPA and AER by restraining GliA activity (**Figure 3**) (Galli et al., 2010; Osterwalder et al., 2014; te Welscher et al., 2002a; Zhulyn et al., 2014). Genetic analyses of unprocessed and/or truncated forms of Gli3 supported that Gli3R is essential for limb AP asymmetry (Cao et al., 2013; Hill et al., 2007; Hill et al., 2009; Wang et al., 2007). In addition, the persistent requirement of *Gli3* for anterior digit patterning are mediated by repressing cell-cycle genes implicated in the proliferative expansion of Shh-dependent mesenchymal progenitors and by terminating BMP antagonist *Gremlin1* (*Grem1*) expression to initiate chondrogenic differentiation (Lopez-Rios et al., 2012; Vokes et al., 2008). Although among Gli derepression genes, *Grem1* is regulated by Gli3R, recent studies of Gli-dependent CRM have revealed that multiple Gli CRMs integrate inputs from Gli, BMP and Shh signaling pathways to regulate asymmetric expression of *Grem1* (Li et al., 2014b; Zuniga et al., 2012).

I-3-3. Interlinked signaling feedback loop between an epithelium and the adjacent mesenchyme

Maintenance and propagation of ZPA-*Shh* expression requires AER-FGF signaling, and vice versa, indicating a positive epithelial-mesenchymal (E-M) feedback loop between the ZPA and the AER (Laufer et al., 1994; Niswander et al., 1994). During this feedback signaling, the BMP antagonist Grem1 is required to relay the Shh signal to the AER and subsequently activates the AER-FGF signaling (Khokha et al., 2003; Michos et al., 2004; Zuniga et al., 1999). Thus, loss-of-function mutation in *Grem1* disrupts the specification and expansion of Shh-dependent distal limb progenitors, which give rise to zeugopod and autopod primordia (Khokha et al., 2003; Michos et al., 2004). By contrast, overexpression of *Grem1* in the limb bud results in polydactyly through inhibition of all BMPs (Bmp2, Bmp4 and Bmp7) (Norrie et al., 2014). This indicates that Grem1-mediated antagonism of BMP activity plays a crucial role in the progression of limb development.

However, other genetic studies revealed that mesenchymal Bmp4 activity is required for the induction of functional AER and initiation of *Grem1* expression in the posterior mesenchyme (Benazet et al., 2009; Nissim et al., 2006). The increase of Grem1-mediated antagonism inhibits BMP activity in the mesenchyme in a self-regulatory manner and low mesenchymal BMP activity persists that is required for the restriction of the AER (Benazet et al., 2009; Selever et al., 2004). Shh-Grem1-FGF feedback loop is self-terminated when the gap between *Shh* descendants and *Grem1* expression domain increases and Shh signaling is subsequently refractory to *Grem1* expression (Benazet et al., 2009; Scherz et al., 2004). Furthermore, the increased AER-FGF signaling contributes to the shutdown of *Grem1* expression and E-M

signaling (Verheyden and Sun, 2008). Consequently, the decrease of Grem1-mediated antagonism leads to a renewed increase in BMP activity during autopod patterning (Benazet et al., 2009; Zeller et al., 2009). This self-regulatory signaling coordinately regulates AP and PD limb bud outgrowth and patterning (**Figure 4**).

When Shh-Grem1-FGF feedback loops are terminated, the increased BMP activity determines definitive digit identity by signaling from the interdigital mesenchyme to the distal phalanx-forming region (Benazet et al., 2009; Dahn and Fallon, 2000; Suzuki et al., 2008; Witte et al., 2010). Furthermore, BMP activity in digit ray development induces programmed cell death of the interdigital mesenchyme (Bandyopadhyay et al., 2006; Maatouk et al., 2009; Pajni-Underwood et al., 2007; Wong et al., 2012). Concurrently, AER-FGF signaling regulates the length and number of phalanges, whereas digit tip forms when FGF signaling stops operating (Sanz-Ezquerro and Tickle, 2003).

Despite of recent progresses in identifying the networks of *trans*-acting regulators interacting with multiple *cis*-regulatory modules orchestrating limb development, the epigenetic control, especially by chromatin remodelers, of the development process is still not understood. Recent studies have reported that *Brg1* and *Snf5* are involved in regulating Hh pathway through interaction with Gli proteins in neural development and tumorigenesis, respectively (Jagani et al., 2010; Zhan et al., 2011). These results indicate the potential involvement of SWI/SNF complex in Shh/Gli-driven limb patterning that requires transcriptional activation, repression and derepression of their target genes.

To define the requirement of SWI/SNF complex in limb patterning, we specifically inactivated *Srg3* in the limb bud mesenchyme using a conditional loss-of-function

Srg3 allele (**Figure 5**) (Choi et al., 2012). Loss of mesenchymal *Srg3*, which could reflect the defects in SWI/SNF complex activity (Sohn et al., 2007), caused the failure to upregulate the expression of *Gli1* and *Ptch1* in the posterior and derepressed them in the anterior mesenchyme after the intact establishment of ZPA. This led us to unravel the bifunctional roles of SWI/SNF complex in limb AP skeletal patterning governed by Shh and Gli3R. Low Shh response and ectopic anterior Hh activity in *Srg3*-deficient limb buds resulted in the loss of AP asymmetry and decreased BMP activity, which was paralleled by the reduction of prechondrogenic progenitors of zeugopod and autopod. In addition, dynamic distribution of *Grem1* in *Srg3*-deficient autopods revealed that Shh responsiveness cooperates with Gli repressor activity to initiate the timely chondrogenesis of digit progenitors. This study illustrates how the bifurcating function of SWI/SNF complex in Hh pathway patterns limb AP skeletal elements.

Figure 2. Vertebrate limb development is controlled by two regulatory signaling centers.

(**A**) Skeletal preparation of mouse forelimb at postnatal day 0 (P0). Abbreviations: cl, clavicle; hu, humerus; ra, radius; sc, scapula; ul, ulna; 1-5, digit number.

(**B**) The expression of *Shh* transcript in the ZPA. Shh drives limb patterning along the anteroposterior axis and is essential for expansion of limb progenitors.

(**C**) The expression of *Fgf8* transcript in the AER. FGF signaling from the AER control the proximodistal limb bud outgrowth.

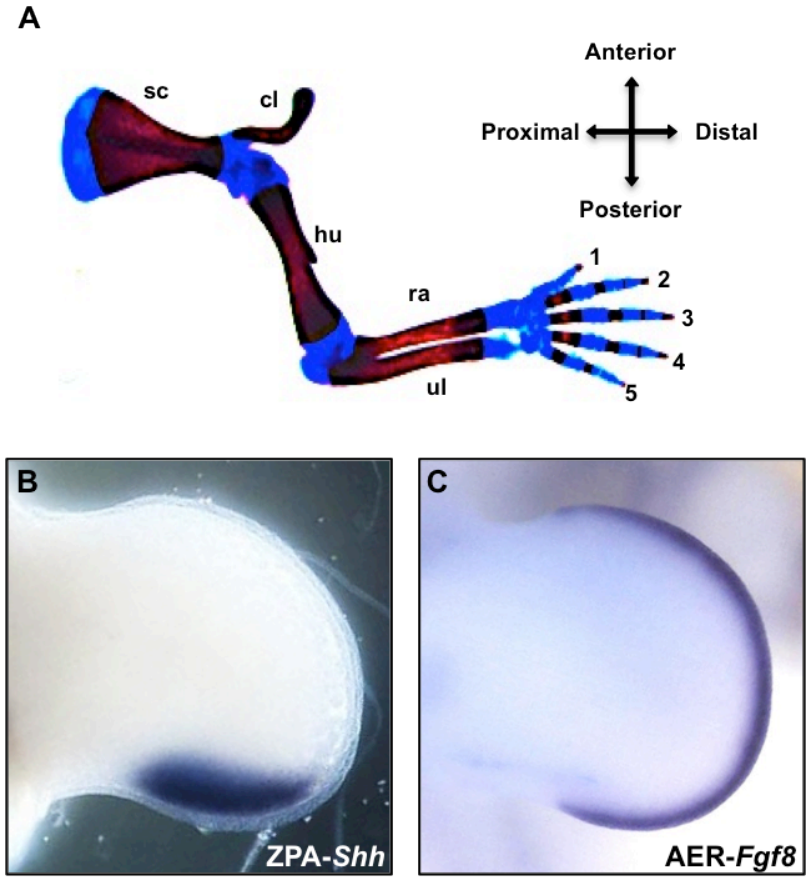
A
Anterior
Proximal
Distal
Posterior
sc
cl
hu
ra
ul
1
2
3
4
5
B
ZPA-Shh
C
AER-Fgf8

Figure 3. Establishment of ZPA and Shh/Gli-dependent limb AP patterning

Prior to *Shh* expression, the antagonistic interaction of transcriptional regulators Gli3 and Hand2 prepatterns the primitive limb field and specifies anterior and posterior limb bud compartments during limb bud protrusion. Transcriptional regulators Hand2 and 5'Hoxd are required for activation of *Shh* expression in the posterior limb bud mesenchyme. The functions of these factors are dependent on Shh activity after the establishment of ZPA. During Shh-dependent phase (E9.5–E12), diffused Shh secreted from the ZPA spatially and temporally generates the graded Shh signaling, and produces the gradients of GliA and GliR along the anteroposterior limb bud axis through inhibition of full-length Gli3 processing. *Shh*-expressing descendants contribute to the specification of digits 3, 4, and 5 and *Gli1*-expressing cells, which respond to Shh, including digit 2 and parts of digit 3 are specified by long-range Shh signaling. In previous studies, digit 1 is regarded as Shh independent but recent works have reported that Shh signaling is detrimental to its formation.

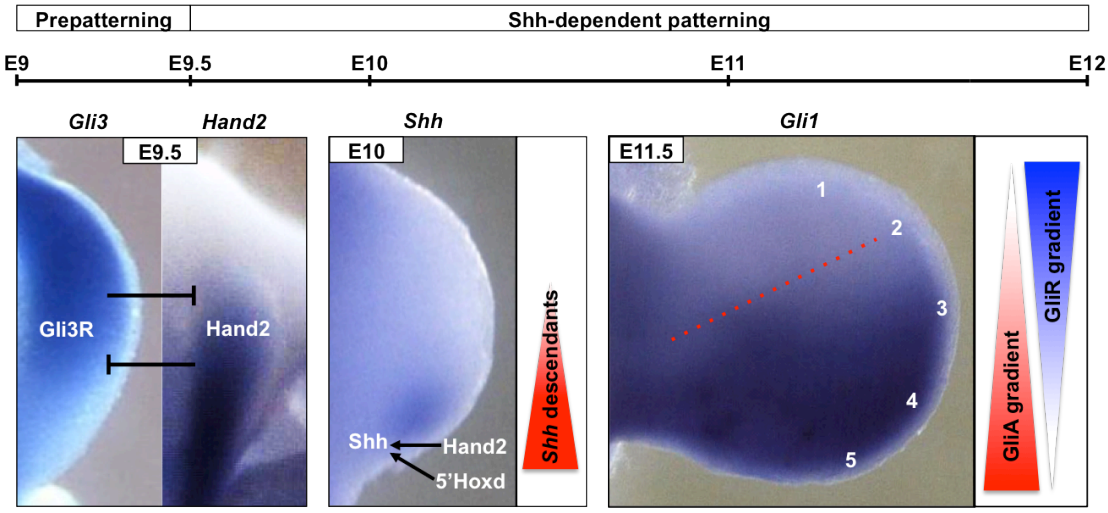
Prepatterning
Shh-dependent patterning
E9
E9.5
E10
E11
E12
Gli3
Hand2
E9.5
Gli3R
Hand2
Shh
E10
Shh
Hand2
5'Hoxd
Shh descendants
Gli1
E11.5
1
2
3
4
5
GliA gradient
GliR gradient

Figure 4. Self-regulatory limb bud signaling system of interlinked feedback loops between an epithelium and the adjacent mesenchyme

(**A**) At initiation phase, *Shh* expression and its signaling are activated independently of Grem1 and FGF. Bmp4 upregulates *Grem1* expression in the posterior mesenchyme and is required to induce AER formation.

(**B**) During propagation phase, increased Grem1 decreases mesenchymal BMP activity, which enables Shh-Grem1-FGF feedback loop and distal progression of limb bud development in a self-regulatory manner. Shh activity upregulates *Grem1* expression and Grem1 strengthens AER and ZPA signaling. At this stage, the induction of *Grem1* by Bmp4 becomes weak and low BMP activity controls the length of AER.

(**C**) Shh-Grem1-FGF feedback loop is self-terminated when the *Shh*-expressing descendants are refractory to *Grem1* expression and increased AER-FGF signaling contributes to the shutdown of *Grem1* expression, indicating the end of E-M signaling. Reduced Grem1-mediated antagonism of BMP activity leads to upregulation of Bmp4.

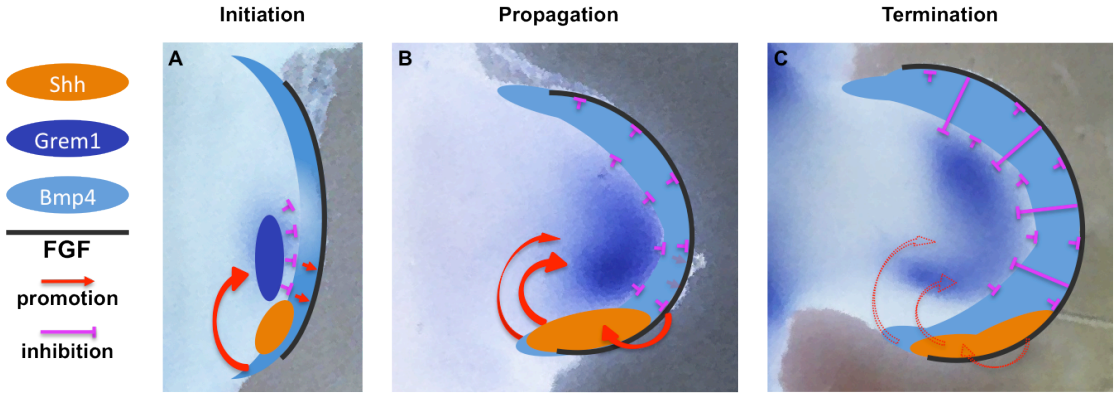
Initiation
Propagation
Termination
A
B
C
Shh
Grem1
Bmp4
FGF
promotion
inhibition

Figure 5. Generation of a conditional loss-of-function *Srg3* allele

Schematic diagram of the targeting strategy. A conditional allele of *Srg3* was generated based on the targeting design of constitutive *Srg3* null allele (Kim et al., 2001), which replaces exon 4 with a *PGK-Neo* gene (neomycin resistant gene). The wild type *Srg3* locus was converted by homologous recombination in mouse embryonic stem cells after electroporation with the targeting vector, which harbors *loxP* (red triangles) both upstream and downstream of exon 4 and *PGK-Neo* (neo) as a selection marker. Targeted cells were selected by G418 and positive ES clones were screened by Southern blot using a probe (red bar). *PGK-Neo* cassette was deleted by Flpase recombination of the *FRT* sites (blue circles). By *Cre-loxP* recombination, the conditional alleles enabled the function of *Srg3* to analyze in specific tissues or at desired developmental stages.

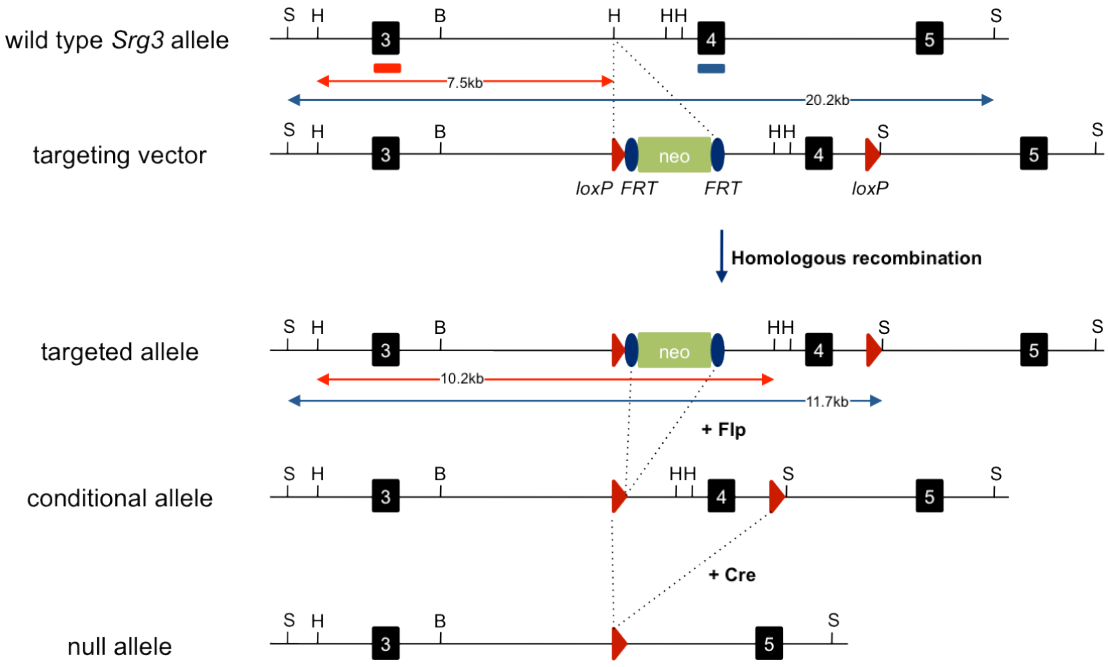
wild type Srg3 allele
S H
3
B
H
HH
4
5
S
7.5kb
20.2kb
targeting vector
neo
loxP FRT
FRT
loxP
Homologous recombination
targeted allele
10.2kb
11.7kb
+ Flp
conditional allele
+ Cre
null allele

II. Materials and Methods

Mice

All mice experiments were approved by Institutional Animal Care and Use Committee (IACUC) of Seoul National University. Generation of mice carrying a conditional allele of *Srg3* (*Srg3*$^{f/f}$) was previously described (Choi et al., 2012). *Srg3*$^{f/f}$, *Msx2-cre* (Sun et al., 2000), *Prx1-cre* (Logan et al., 2002), and *Twist1*$^{f/f}$ mice (Zhang et al., 2010) were bred and maintained on C57BL/6J genetic background. The morning of the day of vaginal plug detection was considered as embryonic day 0.5. The primer sets used to genotype all alleles are listed in **Table 1**.

Quantitative real-time PCR (qPCR) analysis

RNA was purified from samples with TRIzol® reagent according to the manufacturer's instructions (Invitrogen) and reversely transcribed with SuperScript III (Invitrogen) or Quantiscript® Reverse Transcriptase (QIAGEN). cDNA was used for qPCR analysis using SYBR Green PCR mix (Applied Biosystem). The primers used in qPCR analysis were listed in **Table 1**.

Skeletal staining

Skeletal preparations were performed as previously described (Benazet et al., 2009; Galli et al., 2010). For analysis of skeletal structures, samples were prepared and isolated fetuses or euthanized neonates or young pups were optionally stored in tap water at 4°C for 24 h. In the case of neonates sample, to peel off the skin, pups were scalded in hot tap water (65–70°C) for 20–30 sec. After evisceration from the bodies, samples were fixed in 95% ethanol overnight, and transferred into acetone and incubated overnight at room temperature. Samples were briefly washed and stained with Alcian Blue solution (0.05% Alcian Blue 8GX, 20% acetic acid, 80% ethanol)

for 24 h. After washing in 70% ethanol for 6–8 h, samples were transferred into 1% potassium hydroxide and counterstained with Alizarin Red solution (0.03% Alizarin Red, 1% potassium hydroxide). Then, the samples were cleared in 1% potassium hydroxide in 20% glycerol for a few days and stored in glycerol : ethanol (1:1) for imaging.

Whole-mount *in situ* hybridization

The transcript distributions were assessed by whole-mount *in situ* hybridization. Embryos were collected in PBS-0.1% Tween-20 (PBST), fixed in 4% paraformaldehyde (PFA) overnight at 4°C, dehydrated in methanol/PBST series and stored in absolute methanol at -20°C.

Whole-mount *in situ* hybridization was performed according to the standard procedures as described (Piette et al., 2008). Embryos were rehydrated in methanol/PBST reverse series and permeabilized in proteinase K (10 μg/ml) in PBST at room temperature for 11 min (E9.5–E10.5), 14 min (E10.5–E11.5) or 17 min (E11.5–E12.5) for analysis of limb mesenchyme and briefly for 3 min regardless of age for analysis of AER. After washing twice for 5 min in PBST, embryos were fixed in 4% PFA in PBST with 0.2% glutaraldehyde (Sigma). After washing twice for 5 min in PBST, embryos were transferred into 50% hybridization solution (50% (vol/vol) formaldehyde, 1% (wt/vol) blocking reagent, 5X SSC, 1 mg/ml yeast RNA, 0.1% CHAPS, 5mM EDTA) in 50% PBST and then into 100% hybridization solution. Embryos were prehybridized in another 100% hybridization solution for 3 h at 65°C. The labeled probe was added to the translucent embryos and hybridized overnight at 70°C. The hybridization solution with probe was removed and embryos were washed through hybridization solution/2X SSC (pH 4.5) series at 70°C, 2X SSC (pH 7.0) with

0.1% CHAPS at 70°C and MA buffer (100mM maleic acid, 150mM NaCl (pH 7.5)), PBS and PBST. Embryos were incubated in antibody buffer (10% (vol/vol) heat inactivated serum, 1% (wt/vol) blocking reagent, 1X PBST) for at least 2 h at 4°C, transferred into preblocked antibody buffer with anti-digoxigenin antibody and incubated overnight at 4°C with gently rocking. Embryos were rinsed five times in 0.1% BSA in PBST, twice in PBST and twice in AP1 buffer (0.1M NaCl, 0.1M Tris pH 9.5, 50mM $MgCl_2$). Embryos were incubated in BM purple for the appropriate staining time and the staining reaction was halted in stop solution (100mM Tris pH 7.4, 1mM EDTA).

All probes were linearized with the appropriate restriction enzyme and labeled using digoxigenin RNA labeling mix (Roche) with the appropriate polymerase. *Shh*, *Gli1*, *Bmp2*, *Bmp4* and *Bmp7* probes were kindly provided by Y. Kong (Seoul National University). *Fgf4* (Addgene plasmid #22085) (Hebert et al., 1990) and *Fgf8* (Addgene plasmid #22088) (Crossley and Martin, 1995) probes were gifts from G. Martin. Other probes were amplified by PCR from cDNA fragments encompassing at least two exons (about 450~650 bp) of target genes and cloned into pGEM-T vectors (Promega). All representative expression patterns were obtained by analyzing at least three independent embryos per probe. The primers used to amplify cDNA templates for riboprobe synthesis and enzymes treated to generate labeled probes are listed in **Table 2**.

Detection of apoptotic cells

Distribution of apoptotic cells in whole limb buds was analyzed using Lysotracker Red (Molecular Probes L-7528, Invitrogen). Uterus of pregnant female was dissected in prewarmed (37°C) PBS. After the embryonic membranes are removed, embryos

were transferred into prewarmed Lysotracker Red solution (5 μM in PBS) and incubated for 45 min at 37°C. Embryos were washed and fixed overnight in 4% PFA at 4°C. The next day, embryos were dehydrated in a methanol/PBST series and cleared in 50% BBBA solution (2:1, Benzyl Benzoate/Benzyl Alcohol) in 50% methanol for 30 min and 100% BBBA solution for 30 min.

Preparation of mouse embryonic fibroblasts (MEFs)

MEFs were prepared from E13.5-14.5 *Srg3*$^{f/f}$ embryos. The head and internal organs were removed and the torso was minced. These tissues were trypsinized for 30 min at 37°C. Trypsin were added into these partially dissociated tissues and incubated again for 30 min at 37°C. After neutralization with FBS, dissociated MEF were collected by spin down and plated on the 150mm dish.

Chromatin Immunoprecipitation (ChIP)

For ChIP experiments, E11.5 control and *Srg3*$^{f/f}$*;Prx1-cre* limb buds were dissected in cold PBS and minced with a douncer. Disaggregated tissues were crosslinked in 1% formaldehyde (Sigma) for 10 min on a rotator at RT and were lysed for 10 min on ice with SDS lysis buffer (1% SDS, 50mM Tris-Cl (pH 8.1), 10mM EDTA). Lysates were sonicated to an average length of 200-1,000 bp using a Bioruptor sonicator and diluted 10-folds in dilution buffer (20mM Tris-Cl (pH 8.1), 150mM NaCl, 1% Triton X-100, 2mM EDTA). To reduce nonspecific background, samples were precleared for minimally 1 h with salmon-sperm DNA/Protein-A agarose (50% slurry, Millipore). Precleared lysates were incubated overnight on a rotator at 4°C with anti-Brg1, anti-Srg3 or with isotype-control anti-rabbit IgG (Millipore) as a negative control. Washing, elution and reverse-crosslinking of DNA-immunocomplexes and DNA

purification were enriched as previously described (Choi et al., 2012). Purified DNA was analyzed by qPCR with the primers listed in **Table 1**.

Cell Culture

MEF, HEK293T, and Phoenix-eco cells were grown in DMEM (WelGENE) medium supplemented with 10% fetal bovine serum (FBS). For generation of *Srg3*-deficient MEFs, Phoenix-eco packaging cells were transfected with retroviral vectors expressing GFP alone (Empty) as a control or Cre-recombinase (Cre) by calcium phosphate method and retroviral supernatants were harvested 2 d after transfection. MEFs were infected with the retroviral supernatant by spin infection for 90 min at 2500 rpm in the presence of 8 μg/ml polybrene. For Shh pathway activation, HEK293T cells were transiently transfected with ShhN expressing vector (kindly provided by M. Kang, Korea University Guro Hospital). Shh conditioned medium produced from transfected HEK293T cells was replaced with DMEM containing 2% FBS 24 h before harvesting and filtering of medium, and then added to MEFs for 24 h. For inhibition of Hh signaling, MEFs were treated with ethanol vehicle or 5 μM cyclopamine dissolved in vehicle for 24 h. Shh stimulated or cyclopamine treated MEFs were harvested for qPCR.

Immunoprecipitation (IP) and Western Blotting

IP and western blotting were performed as previously described (Choi et al., 2012; Galli et al., 2010). For IP of exogenous Srg3, Gli2 and Gli3, different combinations of Myc-Srg3 (Choi et al., 2012), Flag-Gli2 (Barnfield et al., 2005), HA-Gli3FL and HA-Gli3R (Zhan et al., 2011) were transfected into HEK293T cells. Limb bud or transfected HEK293T protein lysates were immunoprecipitated or detected with

following antibodies: Gli2 (R&D systems), Gli3 (R&D systems), anti-Myc (9E10, Roche), anti-Flag (M2, Sigma), anti-HA (HA-7, Sigma), α-tubulin (Sigma) and rabbit polyclonal IgG (Millipore). Antisera for Brg1 and Srg3 were raised from rabbits in our laboratory. The band density of Gli3R level was quantified using ImageJ software (NIH) and normalized to α-tubulin as a loading control.

Statistical tests

The significance of qPCR analyses was verified by two-tailed nonparametric Mann-Whiney test, calculated using Graphpad Prism 5 software and assumed when p values are less than 0.05.

Table 1. Primers used in this study.

Genotyping

Gene	Forward primer	Reverse primer
Msx2-cre transgene	TTTATTTCAAACGGGGCGGG	GCCGCATAACCAGTGAAACA
Prx1-cre **transgene**	ACCGGCAAACGGACAGAAGCATTT	AGGAGGTAGGAGATTGTGATGGAG
Srg3 **conditional allele**	TGTCATCCATGAGGAGTGGTC	GGTAGCTCACAAATGCCTGT
Twist1 **conditional allele**	AGCGGTCATAGAAAACAGCC	CCGGATCTATTTGCATTTTACCATGGGTCATC

qPCR analysis in limb buds

Gene	Forward primer	Reverse primer
Gapdh	CTACTCGCGGCTTTACGG	TTCGCACCAGCATCCCT
Gli1	CAAGTGCACGTTTGAAG	CAACCTTCTTGCTCACACATGTAAG
Grem1	CCCACGGAAGTGACAGAATGA	AAGCAACGCTCCCACAGTGTA
Ptch1	CTTTTAATGCTGCGACAACTCAGG	CAACACCAAGAGAAGAAACGG
Shh	GATGACTCAGAGGTGCAAAGACAA	TGGTTCATCACAGAGATGGCC

ChIP-qPCR assay

amplicon	Forward primer	Reverse primer
g1	CCGGCACCCCCTCTCTAG	GGCTCTTCCCGCTCACTTC
g2	TTGCTCCCCGCTCTGAATC	CTTGATGCTGTTCCCAAAGCT
p1	ACACACTGGCGCACTATCCA	CCTCAAGCTGCAGCAAATACTG
p2	GAATGGGAGAGGGAGGAAAGAT	GCGGGAGCTCAGTTAGGAAA
p3	TCTTCCAGCATGCTTACCTCTTT	GCTTGGCCGCTGTAATCAAA

Table 2. Primers used to amplify cDNA templates for riboprobe synthesis and enzymes treated to label the probes.

Gene	Forward primer	Reverse primer	Linearization enzyme	RNA Polymerase
Alx4	CTACGCCAAAGAGAGCAACC	CTCATAGGCCGTGGAGAAGT	Sal1	T7
Col2a1	ACACTGGGAATGTCCTCTGC	CACCAGGATTGCCTTGAAAT	Nco1	SP6
Gli3	AGATCCTAAGCCGACAGCAA	TGTCGAACTCTCTGGTGCAG	Sal1	T7
Grem1	CCGCCTCCTGACAAGGCTCAG	TTGGTGGGTGGCTGTAGCTC	Sac1	T7
Hand2	CGAGGAGAACCCCTACTTCC	CCTCTTTCACGTCGGTCTTC	Sal1	T7
Hoxa13	CTACTTCGGCAGCGGCTACT	CTTTGACCCTCCTGTTCTGG	Sac1	T7
Hoxd13	TGGGCTATGGCTACCACTTC	TGTCCTTCACCCTTCGATTC	Sac2	SP6
Msx2	TCAGTCTGCCCTTCCCTA	ATATAAAAAGTCTTATATTTTATTAT	Sac1	T7
Pax9	GCGTGTGCGACAAGTACAAC	GTACTTGGCTTCCTGCTCCA	Sac1	T7
Ptch1	CACCAAGTGATTGTGGAAGC	CACAGCAACAGTCACCGAAG	Sal1	T7
Sox9	ATAAGTTCCCCGTGTGCATC	GTTGGGTGGCAAGTATTGGT	Sac2	SP6
Srg3	CAGCTAGATTCGGTGCGAGT	CCTCTTGTGAGGAAGGATATGG	Sac1	T7

III. Results

***Srg3* is essential for limb anteroposterior patterning**

To study the specific function of *Srg3* in the limb bud mesenchyme, I used a conditional loss-of-function allele of *Srg3* (*Srg3*$^{f/f}$) (Choi et al., 2012) and *Prx1-cre* transgene, which encodes Cre recombinase that is activated in early limb bud mesenchyme (**Figure 6A**,**B**) (Logan et al., 2002). *Prx1-cre*-mediated inactivation of *Srg3* in the limb bud mesenchyme was verified by assessing the expression level of transcript and protein in control and *Srg3*$^{f/f}$;*Prx1-cre* limb buds. Whole-mount RNA *in situ* hybridization for *Srg3* showed its specific clearance throughout the mesenchyme of *Srg3*$^{f/f}$;*Prx1-cre* forelimb buds at embryonic day 9.5 (E9.5) and hindlimb buds at E10.5 (**Figure 6C**). Western blot analysis revealed that Srg3 protein was barely detectable in E10.5 *Srg3*$^{f/f}$;*Prx1-cre* forelimb buds relative to its delayed inactivation in hindlimb buds at the same stage (**Figure 6D**). In addition, the downregulation of Brg1 observed in *Srg3*-deficient limb buds revealed the structural function of Srg3 that stabilizes the SWI/SNF complex (**Figure 6D**) (Sohn et al., 2007).

Srg3$^{f/f}$;*Prx1-cre* mice survived to adulthood but displayed severe limb defects (**Figure 7A**). Skeletal analysis of *Srg3*$^{f/f}$;*Prx1-cre* limbs at birth (P0) revealed the requirement of *Srg3* for limb development. In *Srg3*$^{f/f}$;*Prx1-cre* forelimbs, scapula poorly developed with bifurcated or enlarged foramen, aplastic clavicle, stylopod (humerus) lacking deltoid tuberosity, and radial agenesis were observed (**Figure 7B,C**)

Figure 6. *Prx1-cre*-mediated inactivation of *Srg3* in the limb bud mesenchyme.

(**A**) Mating scheme used to generate *Srg3*$^{f/f}$;*Prx1-cre* embryos.

(**B**) Schematic diagram illustrating the timing of *Prx1-cre* functional activity and *Srg3* inactivation in the forelimb and hindlimb buds.

(**C**) Whole-mount *in situ* hybridization reveals the distribution of *Srg3* transcripts in E9.5 forelimb buds and E10.5 hindlimb buds of control and *Srg3*$^{f/f}$;*Prx1-cre* embryos.

(**D**) Immunoblot analysis of Brg1 and Srg3 proteins in E10.5 forelimb buds and hindlimb buds. The uncleared expression of Srg3 in *Srg3*$^{f/f}$;*Prx1-cre* forelimb buds is likely to be due to its remaining AER expression. α-tubulin was used as loading control.

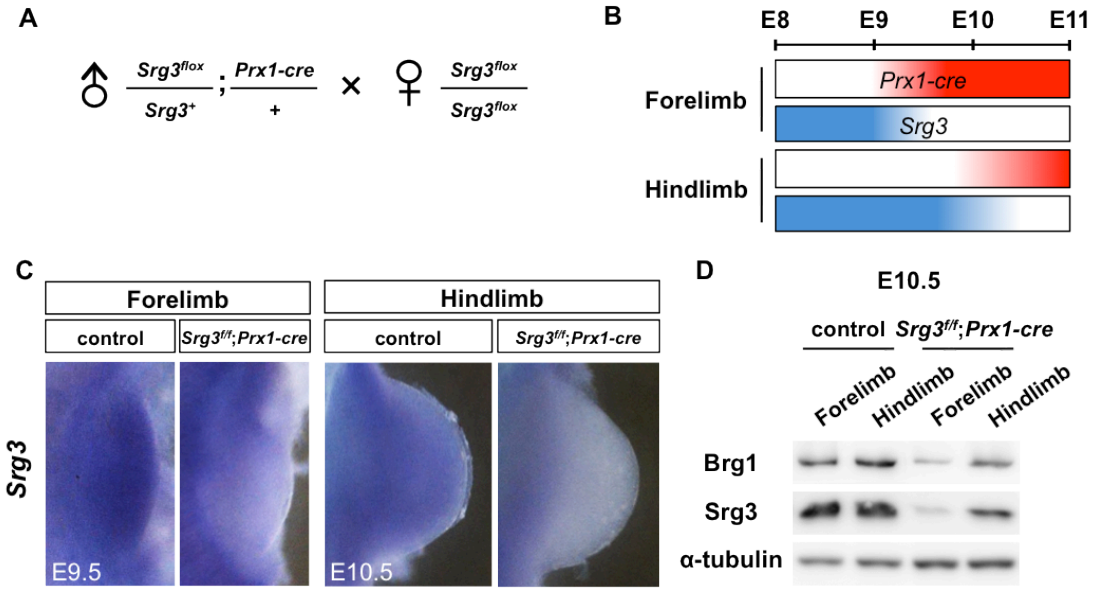
A
Srg3flox / Srg3+ ; Prx1-cre / + × Srg3flox / Srg3flox
B
E8
E9
E10
E11
Forelimb
Prx1-cre
Srg3
Hindlimb
C
Forelimb
Hindlimb
control
Srg3f/f;Prx1-cre
control
Srg3f/f;Prx1-cre
Srg3
E9.5
E10.5
D
E10.5
control
Srg3f/f;Prx1-cre
Forelimb
Hindlimb
Forelimb
Hindlimb
Brg1
Srg3
α-tubulin

Figure 7. *Srg3* is essential for limb anteroposterior patterning.

(A) Gross morphology at postnatal day 0 (P0).

(**B**–**E**) Skeletal preparations of control and *Srg3*$^{f/f}$;*Prx1-cre* forelimbs and hindlimbs of at P0. In (**C**), the inset shows another phenotype of scapula. Red arrowheads denote hypoplastic scapula and black arrowheads indicate loss of clavicle, deltoid tuberosity and radius in *Srg3*$^{f/f}$;*Prx1-cre* forelimb. The insets in (**D**,**E**) show a dorsal view of hindlimb autopod marked with digit numbers. Arrows in (**C**,**E**) point to the fused digits with soft tissues.

(**F**) Skeletal structures of zeugopod elements in hindlimbs of control and *Srg3*$^{f/f}$;*Prx1-cre* pups (P0) and embryos (E14.5). Tibia and fibula were shortened in mutant hindlimbs compared with control.

(**G**) Bright-field images of control and *Srg3*$^{f/f}$;*Prx1-cre* autopods at E16. Arrows indicate syndactyly in the anterior region of *Srg3*-deficient autopods.

Abbreviations: cv, clavicle; dt, deltoid tuberosity; fe, femur; fi, fibula; hu, humerus; pg, pelvic girdle; r, radius; sc, scapula; ti, tibia; u, ulna; 1-5, digit identity.

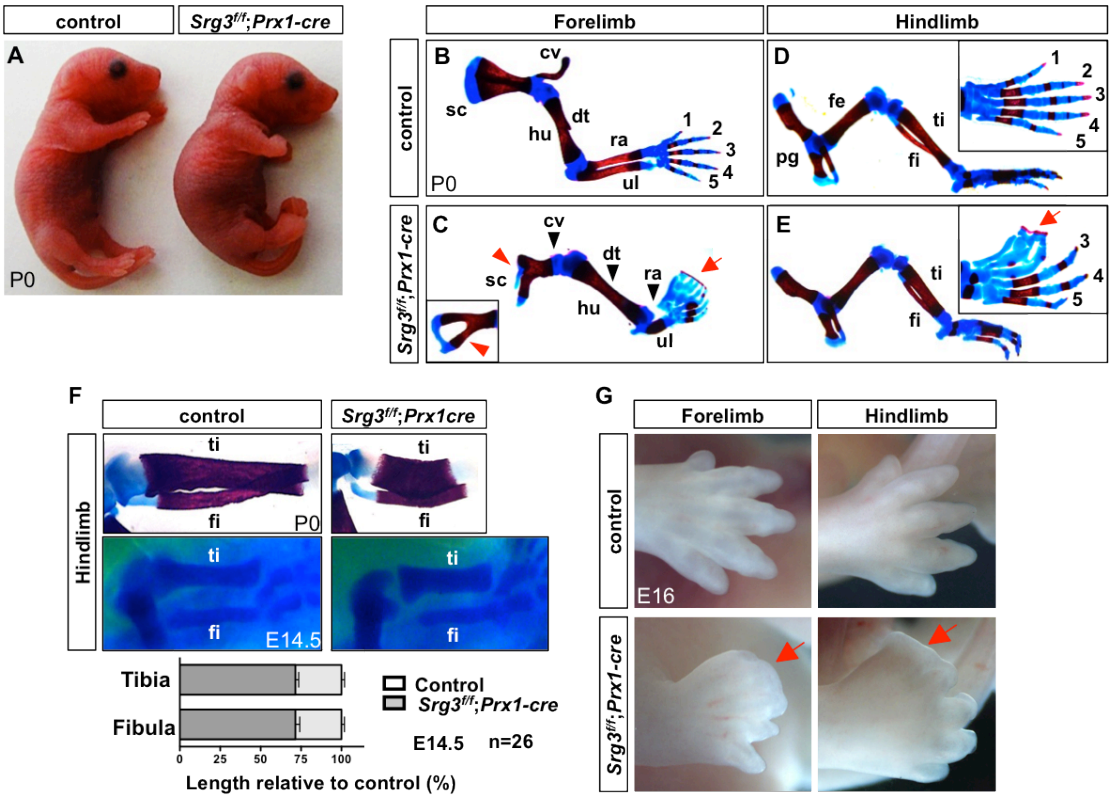
control
Srg3f/f;Prx1-cre
A
P0
Forelimb
Hindlimb
control
Srg3f/f;Prx1-cre
B
cv
sc
dt
hu
ra
ul
1
2
3
4
5
P0
C
D
fe
ti
fi
pg
E
F
control
Srg3f/f;Prx1cre
Hindlimb
ti
fi
P0
E14.5
Tibia
Fibula
0
25
50
75
100
Length relative to control (%)
Control
Srg3f/f;Prx1-cre
E14.5 n=26
G
Forelimb
Hindlimb
control
Srg3f/f;Prx1-cre
E16

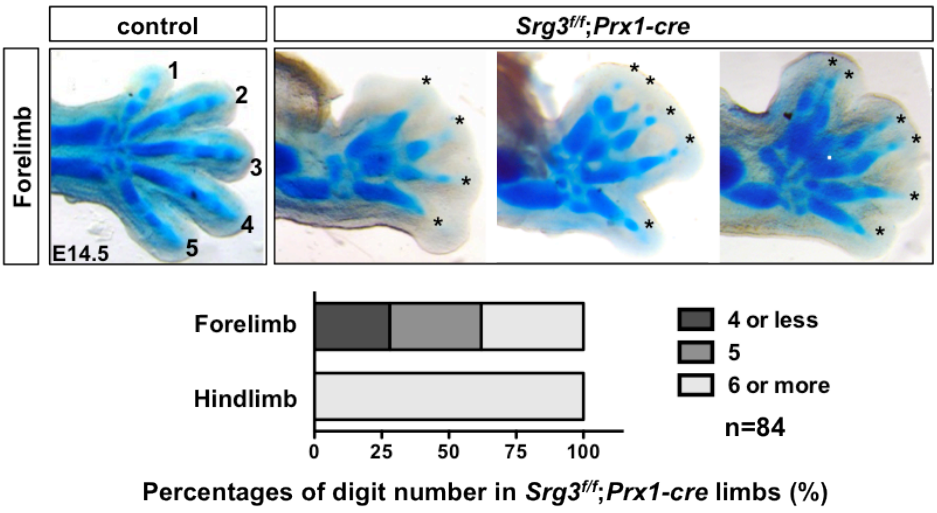

Figure 8. *Srg3* is essential to constrain the developing autopod to pentadactyly.

Percentages of digit number in *Srg3*$^{f/f}$;*Prx1-cre* forelimbs and hindlimbs. *Srg3*$^{f/f}$;*Prx1-cre* hindlimbs predominantly exhibited preaxial polydactyly, whereas their forelimbs displayed various phenotypes in digit numbers. Upper panels show various types of cartilage structures in *Srg3*$^{f/f}$;*Prx1-cre* forelimb digits compared to control. Asterisks indicate digits with uncertain identity.

7B,C). In mutant hindlimbs, the proximal skeletons (pelvic girdle and femur) were retained normally, whereas zeugopod elements (tibia and fibula) were shortened to a similar extent (**Figure 7D–F**). Both *Srg3*$^{f/f}$;*Prx1-cre* forelimbs and hindlimbs had rudimentary digits that were connected by ossified tissues in the anterior digital tips (syndactyly) and exhibited more severe ossification defects in anterior digits than those in posterior ones (**Figure 7C,E,G**). Compared with predominant preaxial polydactyly in *Srg3*$^{f/f}$;*Prx1-cre* hindlimbs, digit number was variable in *Srg3*$^{f/f}$;*Prx1-cre* forelimbs (4 or less, 28%; 5, 34%; 6 or more, 38%, n=84) (**Figure 8**). These results indicated that *Srg3* plays a critical role in restraining the autopod to pentadactyly (five digits). The discrepancy of severity between forelimbs and hindlimbs lacking *Srg3* revealed the temporal requirement for *Srg3* by the onset timing of *Prx1-cre* activity, which is first activated in the prospective forelimb bud prior to hindlimb budding (Logan et al., 2002). Taken together, the asymmetric malformation of zeugopod elements and variable digit numbers observed in *Srg3*-deficienct limbs suggested that mesenchymal *Srg3* was involved in AP patterning.

Srg3$^{f/f}$*;Prx1-cre* forelimb buds establish distinct Hh pathways in the anterior and posterior mesenchyme

Given that the progression of limb bud development requires the formation of ZPA and AER (Zeller et al., 2009), I first analyzed the formation of signaling centers ZPA and AER at early stage. In E10 *Srg3*$^{f/f}$;*Prx1-cre* forelimb buds, ZPA-*Shh* expression was activated without apparent difference compared with control, whereas AER-*Fgf8* expression was slightly reduced (**Figure 9A**). Particularly, the normal expression

level of *Shh* in *Srg3*$^{f/f}$;*Prx1-cre* forelimb buds was confirmed by qPCR (**Figure 9B**). Although inactivation of *Srg3* did not significantly alter the formation of signaling centers, the subtle change of AER suggested the possibility that *Srg3* could function in initial limb development.

To understand the mechanism underlying Srg3-mediated limb AP patterning controlled by the counteraction of Shh and Gli3 (Litingtung et al., 2002; te Welscher et al., 2002b), the expression of Shh/Gli target genes was assessed. In *Srg3*$^{f/f}$;*Prx1-cre* forelimb buds, the expression domains of *Gli1* and *Ptch1* were normal up to at least E10, but were ectopically activated at E10.25 and at E10.75 respectively in the anterior mesenchyme (**Figure 10A–D**). In addition, *Srg3*$^{f/f}$;*Prx1-cre* forelimb buds did not upregulate the expression of *Gli1* and *Ptch1* in the posterior region over time (**Figure 10B,D**). In *Srg3*-deficient hindlimb buds, *Gli1* expression was ectopically activated from around E11, but its posterior restriction was not observed (**Figure 10E,F**). These data suggest that *Srg3* could exert activator and repressor functions in the transcriptional regulation of *Gli1* and *Ptch1* in distinct regions.

To define whether the bipartite function of Srg3 in Hh pathway affects the reciprocal signaling between ZPA and AER (Benazet et al., 2009), I next examined Shh/Grem1/FGF signaling genes during limb bud outgrowth. The distribution of *Shh* transcript in *Srg3*$^{f/f}$;*Prx1-cre* forelimb buds was mildly confined to the posterior mesenchyme but its level remained comparable to control up to at least E10.5 (**Figure 11A,B,E**). The spatially restricted exclusion of *Grem1* expression by Shh activity was observed in the distal posterior of *Srg3*$^{f/f}$;*Prx1-cre* forelimb buds (Scherz et al., 2004), whereas its domain was anteriorly expanded consistently with increase of transcript level (**Figure 11C,D**). The expression domain of *Bmp4* was reduced in the anterior and posterior mesenchyme of *Srg3*$^{f/f}$;*Prx1-cre* forelimb buds (**Figure 11F,G**). In the

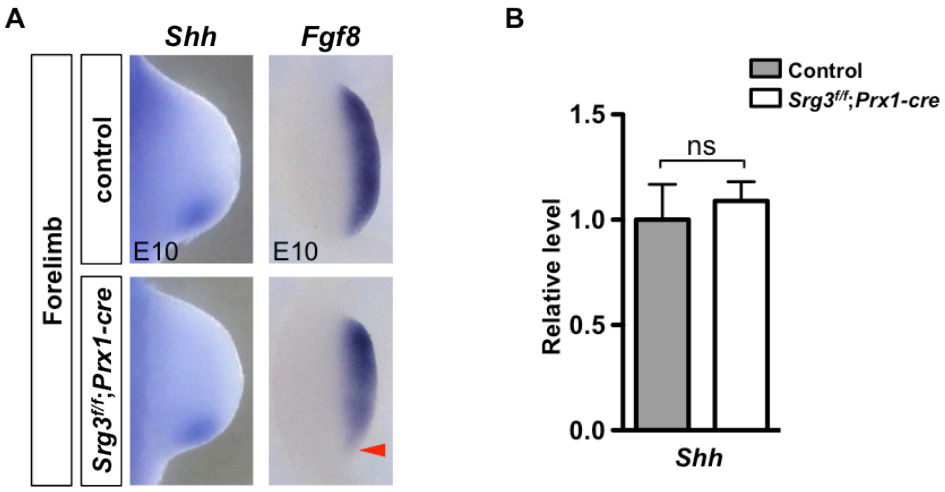

Figure 9. Mesenchymal *Srg3* deficiency does not significantly affect the formation of signaling centers.

(**A**) The expression of *Shh* and *Fgf8* sensing the activity of ZPA and AER, respectively, in control and *Srg3*$^{f/f}$;*Prx1-cre* early limb buds at E10. Arrowhead indicates the reduced activity of AER.

(**B**) Quantitative PCR analysis of *Shh* transcripts in control and *Srg3*$^{f/f}$;*Prx1-cre* at E10. Error bars represent SD from six independent experiments. (ns) not significant.

Figure 10. *Srg3$^{f/f}$;Prx1-cre* forelimb buds establish distinct Hh pathways in the anterior and posterior mesenchyme

(**A**–**D**) The spatiotemporal distribution of *Gli1* and *Ptch1* transcripts in control and *Srg3$^{f/f}$;Prx1-cre* forelimb buds at indicated stages. Dotted lines indicate the boundaries of posterior domain. Arrowheads denote the ectopic expression of Shh target genes in the anterior mesenchyme.

(**E**,**F**) The distribution of *Gli1* transcripts in control and *Srg3$^{f/f}$;Prx1-cre* hindlimb buds. Arrowheads denote anterior ectopic expression.

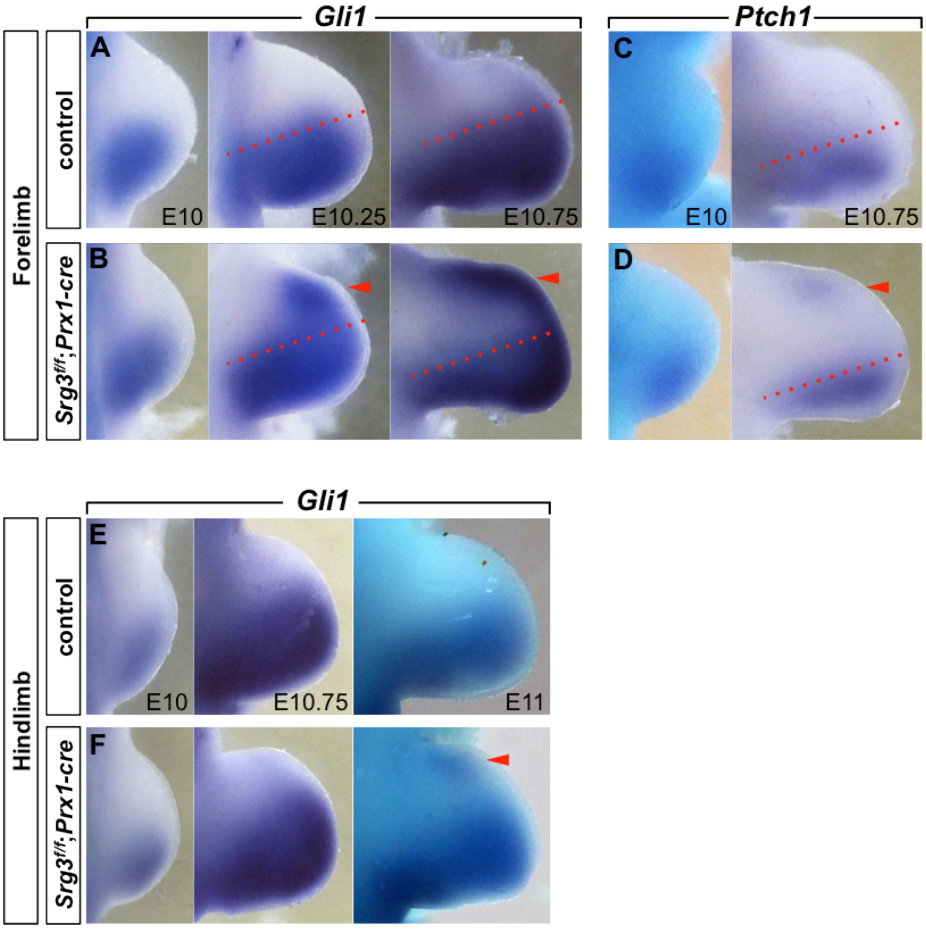
Gli1
Ptch1
Forelimb
control
Srg3f/f;Prx1-cre
A
B
C
D
E10
E10.25
E10.75
Hindlimb
E
F
E11

Figure 11. *Srg3* deficiency differentially alters the epithelial-mesenchymal signaling pathway in the anterior and posterior limb buds.

(**A**–**D**) The spatial distribution of *Shh* and *Grem1* in E10.5 control and *Srg3*$^{f/f}$;*Prx1-cre* forelimb buds. Brackets mark the spatial extent of *Shh* expression domain. Arrowhead in (**D**) indicates the anterior expansion of *Grem1* expression.

(**E**) Quantitative PCR analysis of *Shh* transcript in control and *Srg3*$^{f/f}$;*Prx1-cre* forelimb buds at E10.5. Error bars represent SD from six independent experiments. (ns) not significant; (*)$P<0.05$

(**F**–**K**) The spatial distribution of *Bmp4*, *Fgf4* and *Fgf8* in E10.5 control and *Srg3*$^{f/f}$;*Prx1-cre* forelimb buds. Arrowheads in (**H**–**K**) indicate the anterior and posterior end of AER.

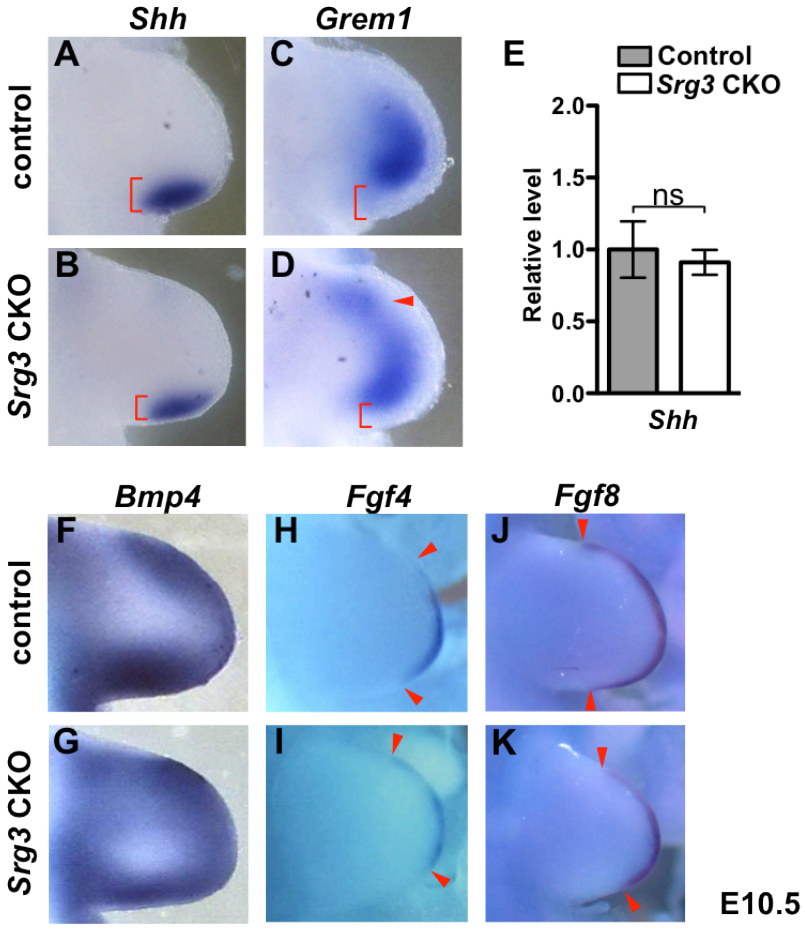
Shh
Grem1
A
C
control
B
D
Srg3 CKO
E
Control
Srg3 CKO
2.0
1.5
1.0
0.5
0.0
Relative level
ns
Shh
Bmp4
Fgf4
Fgf8
F
H
J
control
G
I
K
Srg3 CKO
E10.5

AER, *Fgf4* was anteriorly shifted and *Fgf8* was reduced in the posterior region of *Srg3*$^{f/f}$;*Prx1-cre* forelimb buds, which cause the proximodistal patterning defects in the posterior mesenchyme (**Figure 11H–K**). Taken together, these data suggested that attenuated posterior Shh signaling and anterior ectopic Hh pathway by *Srg3* deficiency differentially affected the spatial distribution of epithelial-mesenchymal signaling genes in the anterior and posterior mesenchyme.

Srg3-containing SWI/SNF complexes are required for transcriptional regulation of *Gli1* and *Ptch1* in developing limb buds

To verify whether Srg3 directly regulates *Gli1* and *Ptch1* expression in developing limbs, I examined the effects of *Srg3* deficiency by transducing a Cre-expressing retroviral vector into *Srg3*$^{f/f}$ MEFs. Real-time quantitative PCR (qPCR) showed *Srg3* deficiency in MEFs enhanced the expression of *Gli1* and *Ptch1*, suggesting that *Srg3* represses Shh target genes (**Figure 12A**). To exclude the possibility that *Srg3* indirectly represses Shh target genes by other factors in MEFs, we treated *Srg3*-deficient MEF cells with Hh pathway inhibitor cyclopamine (Chen et al., 2002). Although cyclopamine reduced the expression of *Gli1* and *Ptch1* in control and *Srg3*-deficient MEFs, *Srg3*-deficient MEFs had a higher level of *Gli1* and *Ptch1* expression than control MEFs (**Figure 12A**). This indicated that Srg3-containing SWI/SNF complex represses Shh/Gli target genes in Hh-free condition. Further, it could corroborate the derepression of Shh/Gli target genes in the anterior mesenchyme of *Srg3*$^{f/f}$;*Prx1-cre* limb buds.

Next, I examined whether *Srg3* is involved in the activation of *Gli1* and *Ptch1*

expression responding to Shh. *Srg3*-deficient MEFs in the presence of Shh-conditioned medium did not sufficiently activate expression of *Gli1* (101- vs. 16.1-fold) and *Ptch1* (7.79- vs. 2.96-fold), compared with control (**Figure 12B**). These data suggested that *Srg3* is required for responding to Shh, supporting the findings that the distribution of *Gli1* and *Ptch1* transcripts was confined to the distal-posterior mesenchyme in forelimb buds lacking *Srg3*.

During limb development, *Gli1* expression requires both transcription factors Gli2 and Gli3 (Bai et al., 2004), and Gli proteins regulate the expression of *Ptch1* (Lopez-Rios et al., 2014; Vokes et al., 2008). I asked whether Srg3 functionally interacts with Gli2 and Gli3 to regulate the expression of *Gli1* and *Ptch1* in developing limbs. Reciprocal coimmunoprecipitation of Srg3 with Gli2 and Gli3 from E11.5 limb bud lysates revealed that Srg3 formed a complex with endogenous Gli2, Gli3FL and Gli3R (**Figure 13A**). In addition, their physical interactions were supported by detection of Myc-tagged Srg3 in Flag-tagged Gli2 and HA-tagged Gli3FL/Gli3R immunoprecipitates from exogenously transfected cells (**Figure 13B**).

Then, Brg1 and Srg3 occupancy at the regulatory regions of *Gli1* and *Ptch1* was assessed by performing chromatin immunoprecipitation followed by qPCR (ChIP–qPCR) assay in E11.5 limb bud extracts. Using functional Gli-binding sites (**Figure 14A,B**) (Vokes et al., 2008), ChIP–qPCR analysis showed that both Brg1 and Srg3 proteins were enriched at the promoter regions of *Gli1* and *Ptch1* around Gli-binding region in control limb buds, whereas their occupancies were significantly diminished in *Srg3*-deficient limb buds (**Figure 14C**). Furthermore, Brg1 and Srg3 were also enriched near the limb specific enhancer of *Ptch1*, which might be required for sensing the graded Shh activity (**Figure 14C, region p3**) (Lopez-Rios et al., 2014). These results suggest that Srg3-containing SWI/SNF complexes are required for the

transcriptional regulation of *Gli1* and *Ptch1* mediated by Gli proteins in developing limbs.

SWI/SNF complex also mediates Hh pathway in the AER

Previous reports have documented that components of Shh signaling transduction are present and Shh signaling pathway is required within the limb bud ectoderm/AER for normal autopod patterning (Bell et al., 2005; Bouldin et al., 2010). To investigate whether *Srg3* also mediates Hh signaling in the AER, *Srg3* was specifically deleted from the AER by using *Msx2-cre* mice (**Figure 15A**) (Mariani et al., 2008; Sun et al., 2000). I focused on the characterization of hindlimb bud, since *Msx2-cre* is active in the prospective AER of hindlimb bud and after AER formation of forelimb bud (**Figure 15B**) (Barrow et al., 2003; Sun et al., 2000). I did not found the clearance of *Srg3* transcript in the AER of *Srg3*$^{f/f}$;*Msx2-cre* hindlimb buds due to the defects in AER formation or the limit of *in situ* hybridization detection, whereas AER-Srg3 protein was almost undetectable in *Srg3*$^{f/f}$;*Msx2-cre* hindlimb buds at around E11.0 (**Figure 15C,D**).

Next, the distribution of *Gli1* transcripts was analyzed by whole mount *in situ* hybridization. In *Srg3*$^{f/f}$;*Msx2-cre* hindlimb buds, *Gli1* expression was significantly activated in the distal tips excluding the posterior-most regions compared to control (**Figure 16A,B**). Interestingly, the expression of *Ptch1* in *Srg3*$^{f/f}$;*Msx2-cre* hindlimb buds was not significantly affected in the distal margin, but mildly upregulated in the mesenchyme (**Figure 16C,D**). The expression domain of *Shh* was maintained within the normal area but gently dispersed in *Srg3*$^{f/f}$;*Msx2-cre* hindlimb buds (**Figure**

16E,F). This likely resulted from the attenuated sensing by low Ptch1 in the posterior AER. Taken together, these data indicated that *Srg3* mediates the AER-Hh signaling.

Mesenchymal *Srg3*-deficient forelimb buds lead to progressive loss of AP asymmetry

In *Srg3*-deficient forelimb buds, normal *Shh* expression up to at least E10 appears to specify the intact AP axis, which requires the early and transient function of polarizing activity (Zhu et al., 2008). I determined whether bipartitely regulated Hh signaling in mutant forelimb buds contributes to the molecular AP asymmetry. The expression domains of posterior marker *Hand2* and anterior marker *Gli3* that establish AP polarity at prepatterning stage were normally retained at E9.5 in *Srg3*$^{f/f}$;*Prx1-cre* forelimb buds (**Figure 17A–D**) (Galli et al., 2010; te Welscher et al., 2002a). The distribution of posterior markers *Hand2* and *Hoxd13* was not significantly affected up to at least E10.25, but expanded into the anterior region at E10.75 in *Srg3*$^{f/f}$;*Prx1-cre* forelimb buds (**Figure 18A–D**). By contrast, in the posterior aspect, *Hand2* expression was reduced and posteriorly confined, and *Hoxd13* expression remained low in *Srg3*$^{f/f}$;*Prx1-cre* forelimb buds, similarly to *Gli3*-deficient limb buds (**Figure 18B,D**) (Galli et al., 2010). To determine whether *Srg3*$^{f/f}$;*Prx1-cre* forelimb buds retain anterior identity, I assessed expression of anterior markers *Alx4* and *Pax9* (Li et al., 2014a) and found the progressive decrease of *Alx4* and abolition of *Pax9* in *Srg3*$^{f/f}$;*Prx1-cre* forelimb buds (**Figure 18E–H**). Consistently, the expression of anterior markers was mildly downregulated in *Srg3*$^{f/f}$;*Prx1-cre* hindlimb buds, suggesting that loss of anterior identity in *Srg3*-deficient limb buds correlates with the

timing of *Srg3* inactivation (**Figure 19**). Taken together, these data indicated that *Srg3* deficiency progressively posteriorized the anterior mesenchyme, leading to disruption of asymmetry after early specification of AP axis.

Mesenchymal *Srg3* deficiency induces ectopic *Shh* expression and distalizes epithelial-mesenchymal signaling during progression of limb development

Inactivation of *Srg3* in the limb bud mesenchyme caused the progressive alterations in both *Gli1* and *Ptch1* expression as well as those in AP identities (**Figures 10, 18,** and **19**). To gain further insights into the concurrent regulation of *Gli1* and *Ptch1* by SWI/SNF complex, I reexamined the distribution of Shh responsive genes at subsequent stages. By E11.5, *Gli1* and *Ptch1* were activated in a graded manner along the AP axis in control forelimb buds, whereas their expression domains including ectopic regions were confined to the distal region in *Srg3*-deficient forelimb buds (**Figure 20A–D**). Importantly, *Ptch1* transcripts were not detected in the core mesenchyme of *Srg3*-deficient forelimb buds (**Figure 20D**). The low response to Shh was not observed in mutant hindlimb buds that had enough time to pattern posterior progenitors by Shh signaling (**Figure 20E–H**).

In *Srg3*$^{f/f}$;*Prx1-cre* forelimb buds, *Shh* expression was ectopically induced in the anterior margin at E11.0 and expanded along the distal margin at E11.5 (**Figure 21A–D**). Ectopic and anterior expansion of *Shh* expression was observed at E11.5 and E12 in mutant hindlimb buds, respectively (**Figure 21E–H**). These data indicated that *Srg3* was required for defining the range of Shh signaling in mesenchymal cells responding to Shh and subsequently maintaining localized *Shh* expression. Ectopic

Shh signaling reduced Gli3R protein level by inhibiting the processing of Gli3 and altered the ratio of Gli3FL/Gli3R in the anterior mesenchyme of *Srg3*$^{f/f}$;*Prx1-cre* forelimb buds (**Figure 22**).

After ectopic *Shh* was induced, the anteriorly expanded domain of *Grem1* at E10.5 was divided into two parts, the anterior domain and the posterior domain (**Figures 11D** and **23A,B**). In E11.5 *Srg3*$^{f/f}$;*Prx1-cre* forelimb buds, the anterior derepressed domain of *Grem1* expression was remarkably reduced in the distal mesenchyme, whereas its posterior domain was distally shifted (**Figure 23B**). As the posterior domain of *Grem1* closer to the AER reflects loss of FGF signaling repressing *Grem1* (Verheyden and Sun, 2008), I assessed AER-*Fgf8* expression and found the thinning and posterior loss of AER together with ectopic upregulation in the anterior end (**Figure 23C,D**). *Hoxd13* expression was also anteriorly expanded and confined to the distal mesenchyme in *Srg3*$^{f/f}$;*Prx1-cre* forelimb buds (**Figure 23E,F**). In *Srg3*-deficient hindlimb buds, the expression of *Grem1*, *Fgf8* and *Hoxd13* was ectopically upregulated in the anterior margin (**Figure 23G–L**). Particularly, the distalization of *Grem1* and *Hoxd13* expression domains was also observed in *Srg3*-deficient hindlimb buds, although to a lesser extent than in forelimb buds (**Figure 23H,L**). These data revealed that low response to Shh from the ZPA and ectopic anterior Hh pathway activity by *Srg3* deficiency distalized epithelial-mesenchymal signaling and expanded the anterior digit progenitors.

Figure 12. *Srg3* is required for transcriptional regulation of *Gli1* and *Ptch1* in the embryonic fibroblasts.

(**A**) Quantitative PCR analysis of *Gli1* and *Ptch1* mRNA in $Srg3^{f/f}$ MEF infected with empty vector (Empty) or Cre-expressing viral vector (Cre). Each of infected MEFs was treated with ethanol vehicle (EtOH) or cyclopamine (Cyc).

(**B**) Quantitative PCR analysis of *Gli1* and *Ptch1* mRNA in $Srg3^{f/f}$ MEF infected with empty vector (Empty) or Cre-expressing viral vector (Cre). Each of infected MEFs was incubated in Shh-conditioned media (+) or control media (−). Error bars represent SD from six independent experiments. (*)$P<0.05$; (**)$P<0.01$.

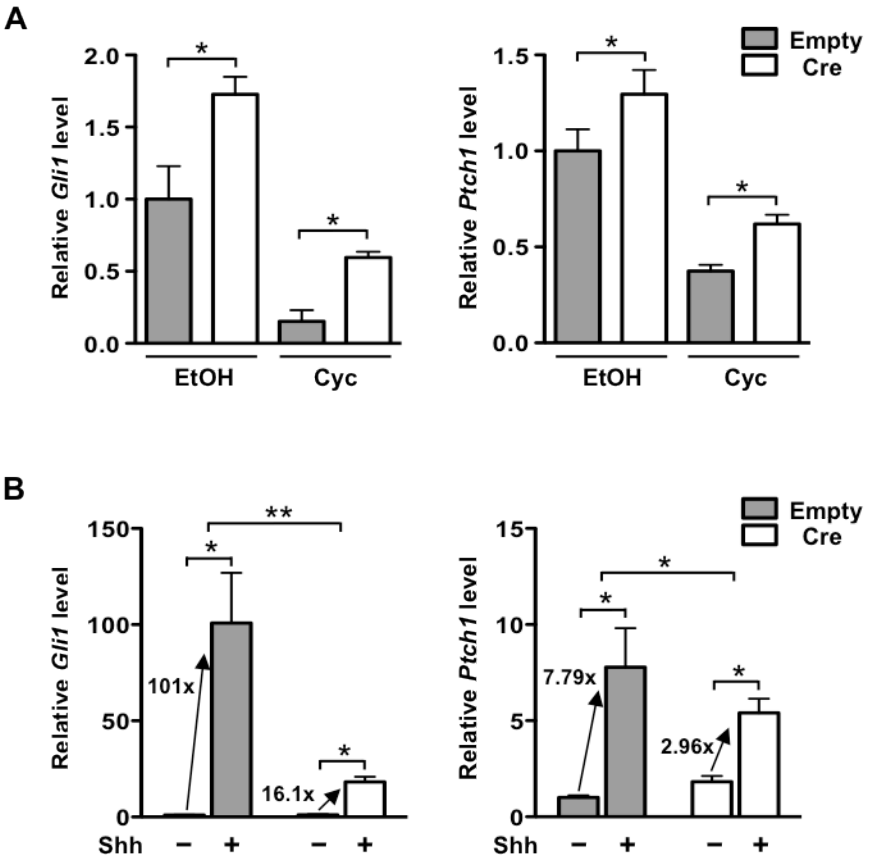
A
Relative Gli1 level
2.0
1.5
1.0
0.5
0.0
*
*
EtOH
Cyc
Relative Ptch1 level
1.5
1.0
0.5
0.0
*
*
Empty
Cre
EtOH
Cyc
B
Relative Gli1 level
150
100
50
0
**
*
*
101x
16.1x
Shh
–
+
–
+
Relative Ptch1 level
15
10
5
0
*
*
*
7.79x
2.96x
Empty
Cre
Shh
–
+
–
+

Figure 13. *Srg3* directly interacts with bifunctional Gli proteins in the developing limbs.

(**A**) Reciprocal immunoprecipitation of Srg3 with Gli2 and Gli3 proteins in E11.5 control limb buds.

(**B**) Immunoprecipitation with anti-Myc of HEK293T cell lysates exogenously transfected with Myc-Srg3 and Flag-Gli2 (top) or with Myc-Srg3, HA-Gli3FL and HA-Gli3R (bottom).

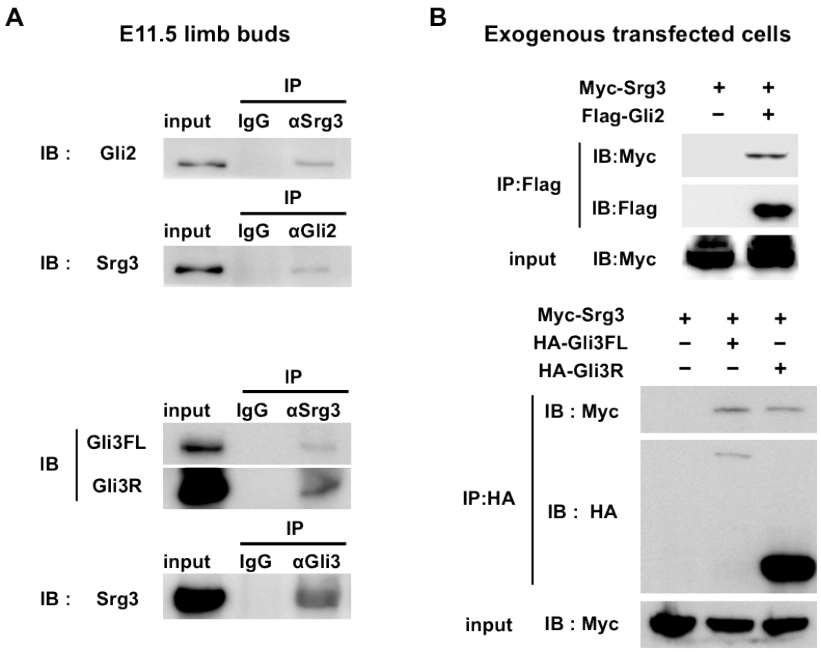
A
E11.5 limb buds
IP
input
IgG
αSrg3
IB :
Gli2
IP
input
IgG
αGli2
IB :
Srg3
IP
input
IgG
αSrg3
IB
Gli3FL
Gli3R
IP
input
IgG
αGli3
IB :
Srg3
B
Exogenous transfected cells
Myc-Srg3 + +
Flag-Gli2 − +
IP:Flag
IB:Myc
IB:Flag
input
IB:Myc
Myc-Srg3 + + +
HA-Gli3FL − + −
HA-Gli3R − − +
IP:HA
IB : Myc
IB : HA
input
IB : Myc

Figure 14. Brg1 and Srg3 occupy the regulatory regions of *Gli1* and *Ptch1* in the developing limb.

(**A,B**) Schematic representation of the relative positions of primer sets in the *Gli1* locus (*g1*, *g2*) (**A**) and *Ptch1* locus (*p1–p3*) (**B**) around the putative Gli-binding sites (green peaks). Direction of transcription (arrows) and exons (numbers above boxes) are indicated.

(**C**) ChIP–qPCR analysis of DNA fragments precipitated with anti-Brg1 (*b*), anti-Srg3 (*s*) and IgG (*i*) in E11.5 control and *Srg3*$^{f/f}$;*Prx1-cre* limb buds. All data are represented as the percentages of input DNA. Error bars represent SD from three independent experiments.

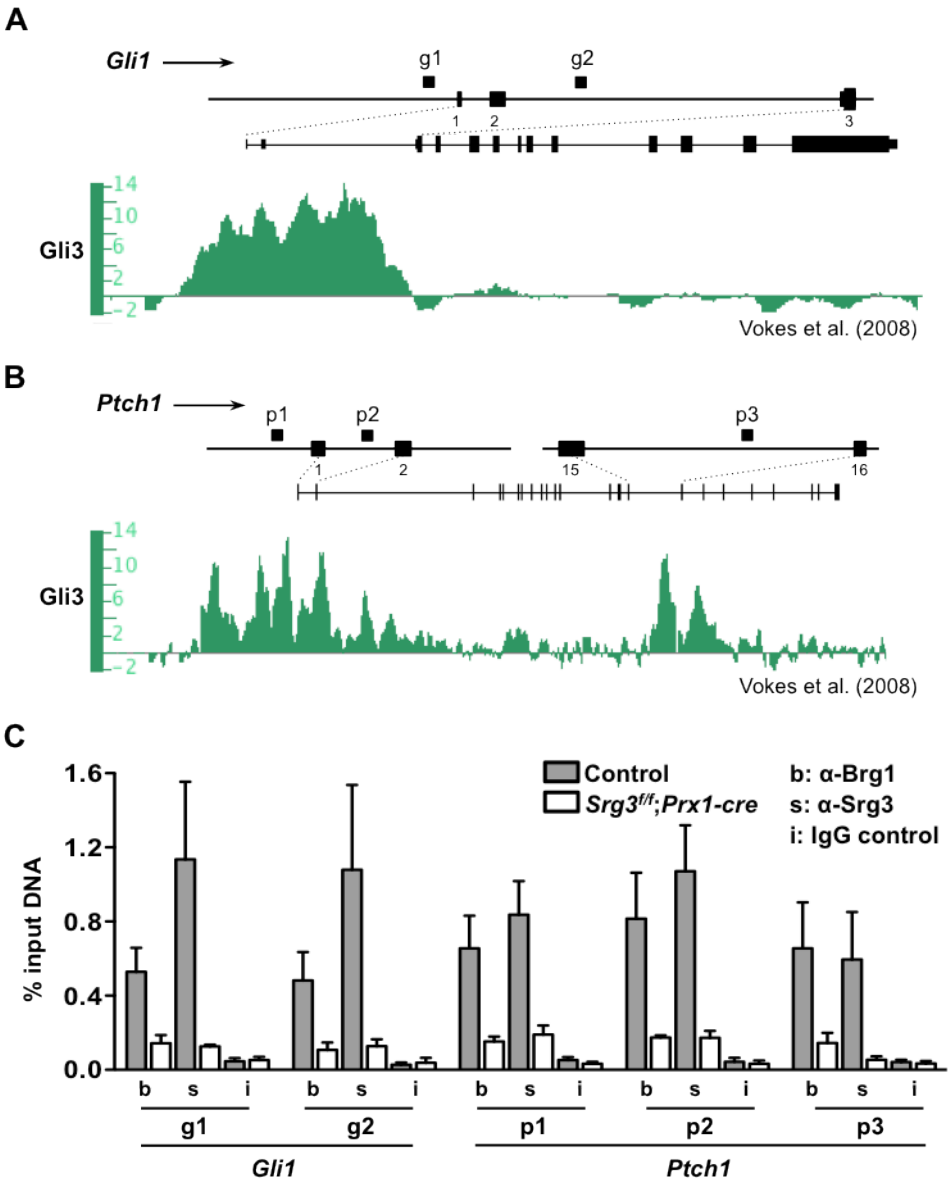
A
Gli1
g1
g2
1
2
3
Gli3
14
10
6
2
−2
Vokes et al. (2008)
B
Ptch1
p1
p2
p3
1
2
15
16
Gli3
14
10
6
2
−2
Vokes et al. (2008)
C
Control
Srg3f/f;Prx1-cre
b: α-Brg1
s: α-Srg3
i: IgG control
% input DNA
1.6
1.2
0.8
0.4
0.0
b s i b s i b s i b s i b s i
g1
g2
p1
p2
p3
Gli1
Ptch1

Figure 15. *Msx2-cre*-mediated inactivation of *Srg3* in the limb bud ectoderm.

(**A**) Mating scheme used to generate *Srg3*$^{f/f}$;*Msx2-cre* embryos.

(**B**) Schematic diagram illustrating the timing of *Msx2-cre* functional activity and *Srg3* inactivation in the forelimb and hindlimb buds.

(**C**) Whole-mount *in situ* hybridization reveals the distribution of *Srg3* transcripts in E10.5 hindlimb buds of control and *Srg3*$^{f/f}$;*Msx2-cre* embryos.

(**D**) Immunohistochemistry of Srg3 proteins in E10.5 control and *Srg3*$^{f/f}$;*Msx2-cre* hindlimb buds.

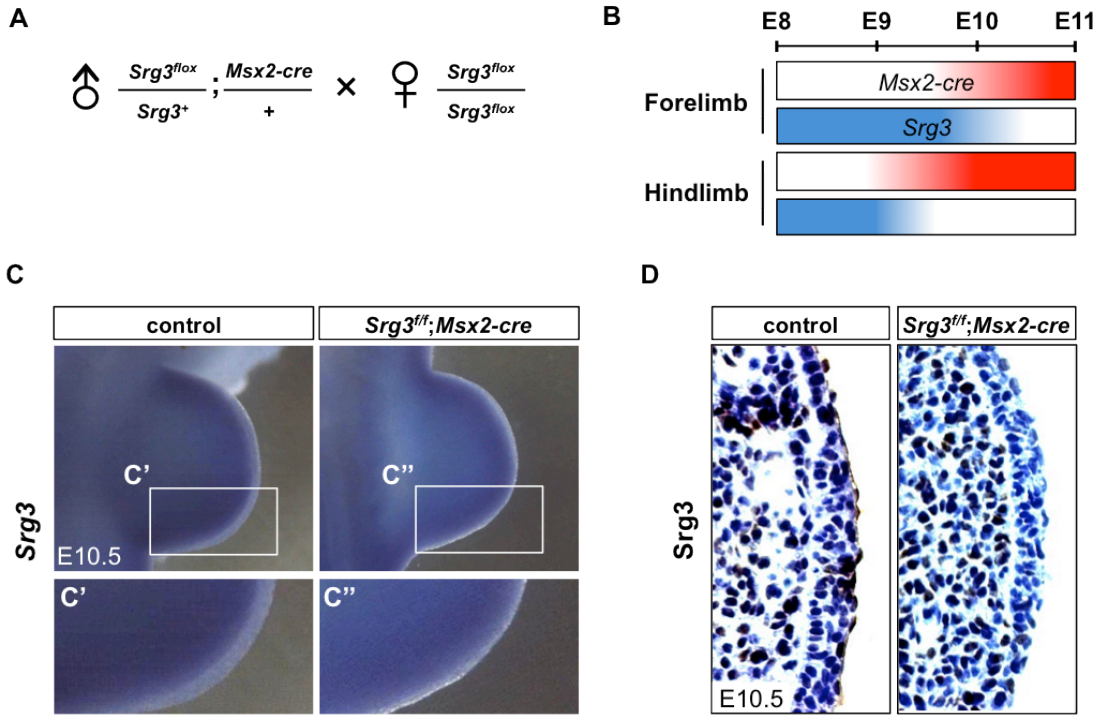
A
♂ Srg3flox / Srg3+ ; Msx2-cre / + × ♀ Srg3flox / Srg3flox
B
E8
E9
E10
E11
Forelimb
Hindlimb
Msx2-cre
Srg3
C
control
Srg3f/f;Msx2-cre
Srg3
C'
C''
E10.5
D
control
Srg3f/f;Msx2-cre
Srg3
E10.5

Figure 16. SWI/SNF complex also mediates Hh pathway in the AER.

(**A,B**) Spatiotemporal distribution of Hh target gene *Gli1* transcripts in control and *Srg3*$^{f/f}$;*Msx2-cre* hindlimb buds at indicated stages.

(**C–F**) Distribution of *Ptch1* and *Shh* in control and *Srg3*$^{f/f}$;*Msx2-cre* hindlimb buds at indicated stages.

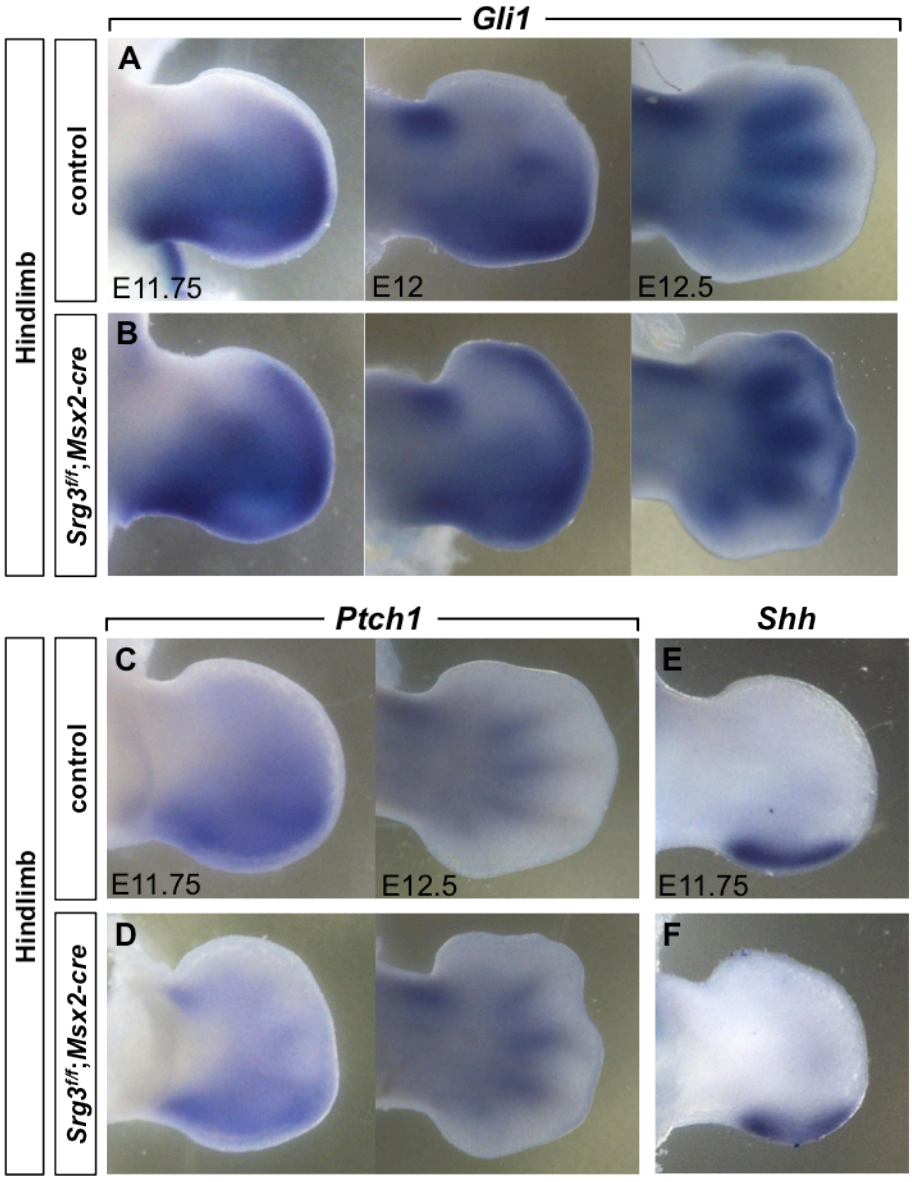
Gli1
Hindlimb
control
A
E11.75
E12
E12.5
Srg3f/f;Msx2-cre
B
Ptch1
Shh
C
E11.75
E12.5
D
E
E11.75
F

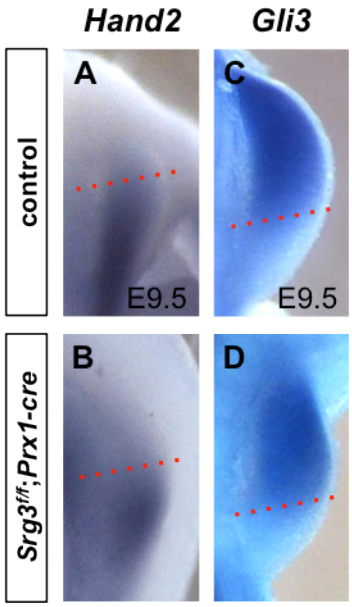

Figure 17. *Srg3*$^{f/f}$*;Prx1-cre* forelimb buds establish the intact AP axis.

(**A–D**) Distribution of *Hand2* and *Gli3* transcripts in E9.5 control and *Srg3*$^{f/f}$*;Prx1-cre* forelimb buds. Dotted lines indicate the boundary of expression domains.

Figure 18. *Srg3* is required for the maintenance of anteroposterior identity in the developing limb.

(**A**–**D**) Spatiotemporal distribution of posterior markers *Hand2* and *Hoxd13* in control and *Srg3*$^{f/f}$;*Prx1-cre* forelimb buds at indicated stages. Dotted lines indicate the boundary of posterior expression domain. Arrowheads indicate the anterior expansion of *Hand2* and *Hoxd13*.

(**E**–**H**) Distribution of anterior markers *Alx4* and *Pax9* in control and *Srg3*$^{f/f}$;*Prx1-cre* forelimb buds at indicated stages.

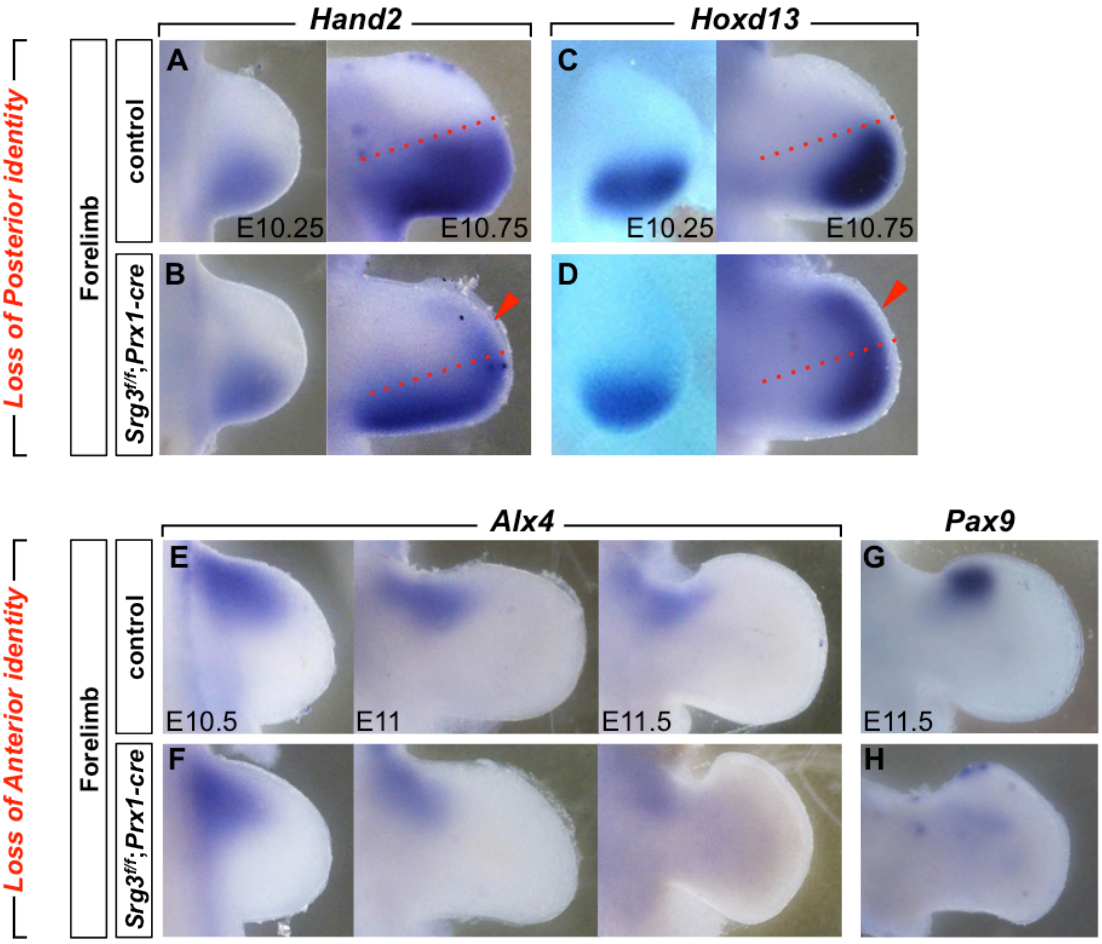
Hand2
Hoxd13
Loss of Posterior identity
Forelimb
control
Srg3f/f;Prx1-cre
A
B
C
D
E10.25
E10.75
E10.25
E10.75
Alx4
Pax9
Loss of Anterior identity
Forelimb
control
Srg3f/f;Prx1-cre
E
F
G
H
E10.5
E11
E11.5
E11.5

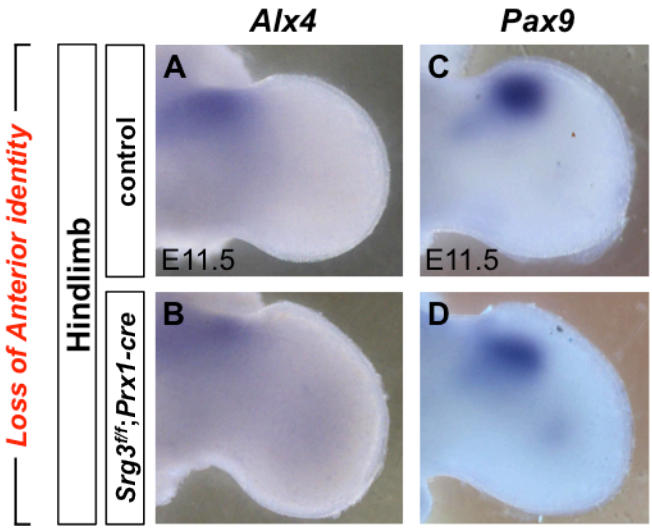

Figure 19. *Srg3*$^{f/f}$*;Prx1-cre* hindlimb buds retain the anterior identity to a low extent.

(**A**–**D**) Spatiotemporal distribution of anterior markers *Alx4* and *Pax9* in control and *Srg3*$^{f/f}$*;Prx1-cre* hindlimb buds at E11.5.

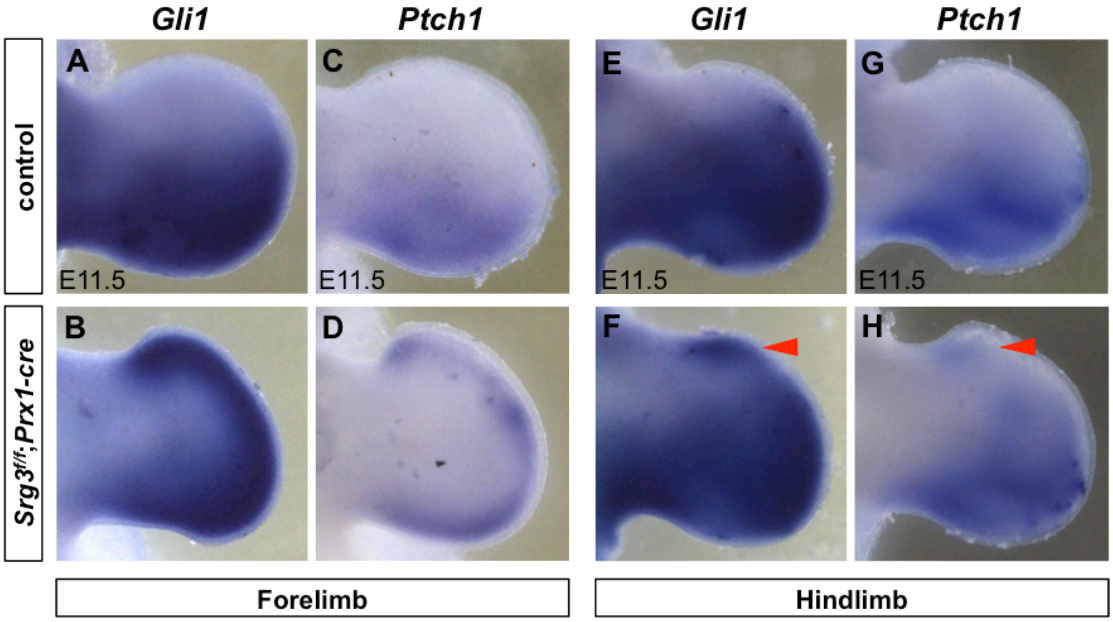

Figure 20. Mesenchymal *Srg3* deficiency causes the defects in long-range Shh signaling in the mesenchyme.

(**A**–**H**) Distribution of Gli1 and Ptch1 in E11.5 control and *Srg3*$^{f/f}$;*Prx1-cre* forelimb and hindlimb buds. Arrowheads indicate the anterior ectopic expression of Shh target genes.

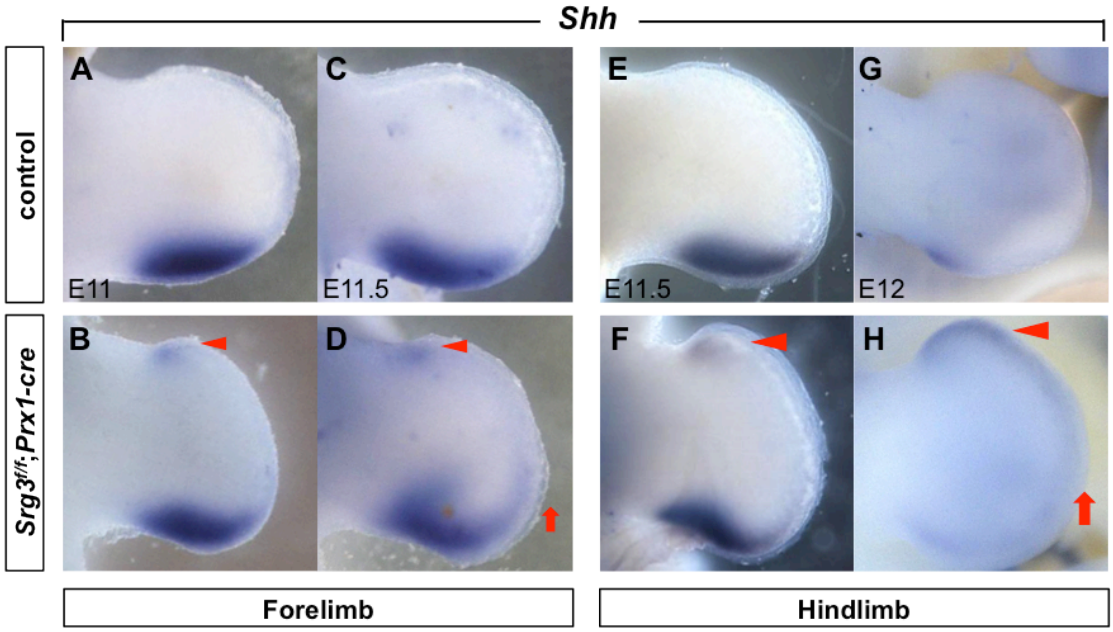

Figure 21. Mesenchymal *Srg3* deficiency induces ectopic and anteriozed *Shh* expression.

(**A**–**H**) Spatial distribution of *Shh* transcripts in control and *Srg3*$^{f/f}$;*Prx1-cre* forelimb and hindlimb buds at indicated stages. Arrowheads and arrows indicate the anterior ectopic expression and anterior expansion of *Shh*, respectively.

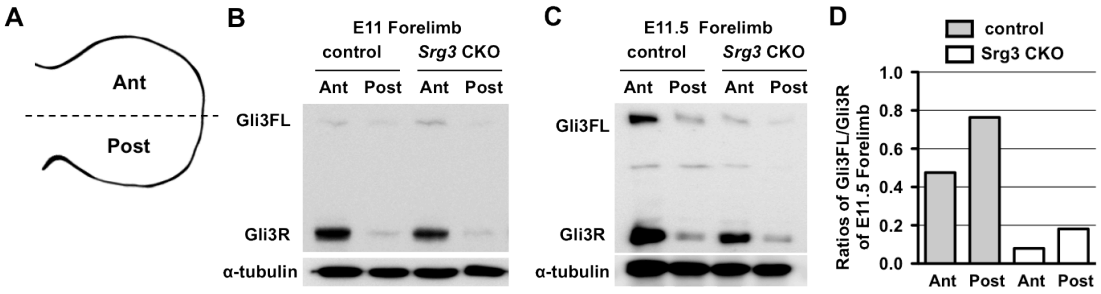

Figure 22. Ectopic *Shh* expression inhibits Gli3 processing in the anterior mesenchyme.

(**A**) Control and *Srg3*$^{f/f}$;*Prx1-cre* forelimb buds at E11 were dissected into anterior (Ant) and posterior (Post) halves as diagrammed.

(**B,C**) Western blot analysis of Gli3FL and Gli3R in lysates from the anterior (Ant) and posterior (Post) halves of E11 control and *Srg3*$^{f/f}$;*Prx1-cre* forelimb buds. Values represent the relative levels of Gli3R protein. α-tubulin served as a loading control.

(**D**) Ratio of Gli3FL/Gli3R in E11.5 control and *Srg3*$^{f/f}$;*Prx1-cre* forelimb buds.

Figure 23. Mesenchymal *Srg3* deficiency distalizes epithelial-mesenchymal signaling during progression of limb development.

(**A**–**L**) Distribution of *Grem1*, *Fgf8* and *Hoxd13* transcripts in control and *Srg3*$^{f/f}$;*Prx1-cre* forelimb and hindlimb buds at indicated stages. The distance between posterior domain of *Grem1* and AER (brackets), the posterior end of AER (black arrowheads), and the distalized domain of *Hoxd13* (asterisk) are indicated. Red arrowheads point to the anterior ectopic expression.

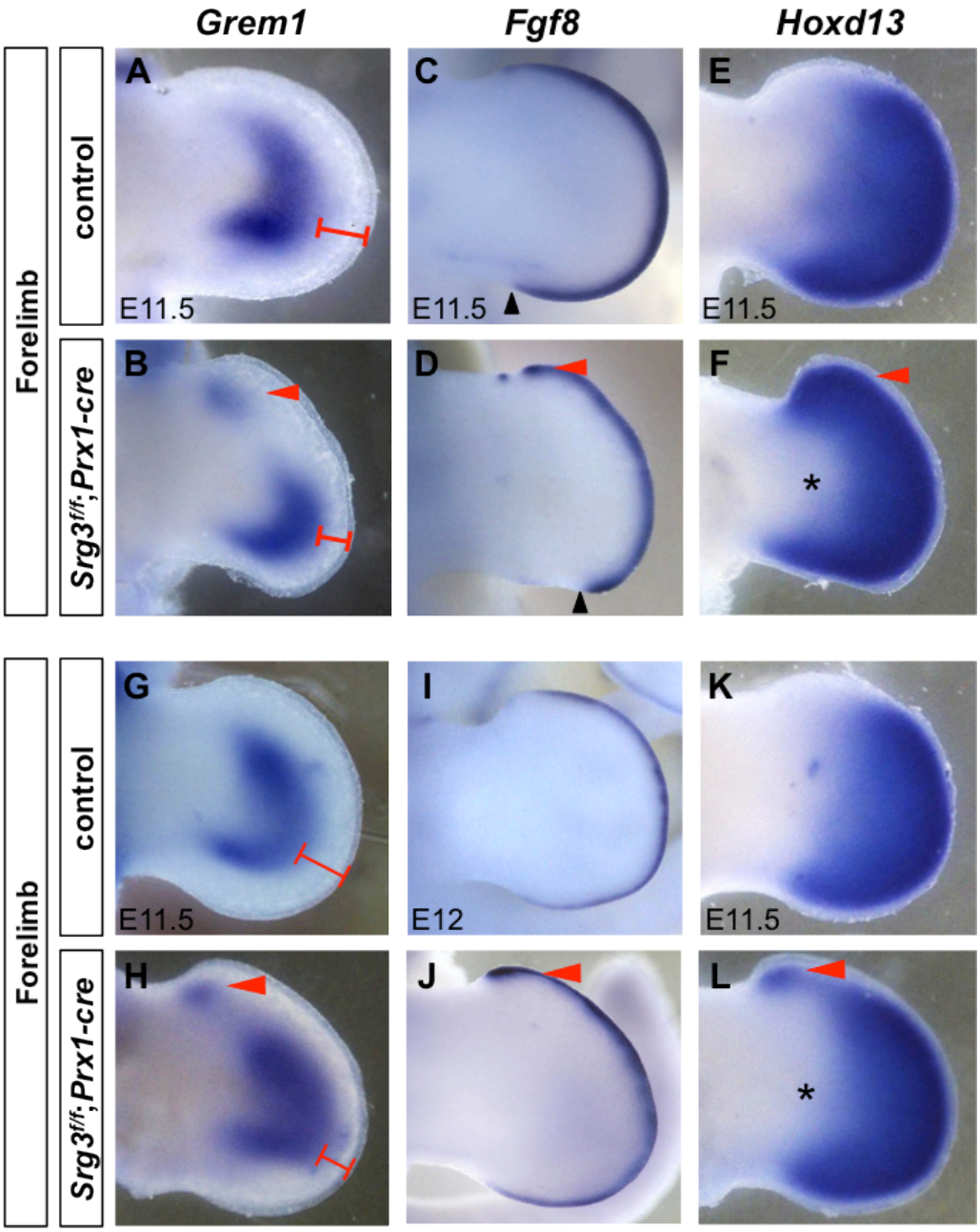
Grem1
Fgf8
Hoxd13
Forelimb
control
Srg3f/f;Prx1-cre
A
B
C
D
E
F
G
H
I
J
K
L
E11.5
E11.5
E11.5
E11.5
E12
E11.5
*
*

Disrupted BMP signaling and defective chondrogenesis in forelimb buds lacking mesenchymal *Srg3*

Posterior Shh signaling establishes limb skeletal structures including posterior zeugopod elements (ulna/fibula) and digits 2 to 5 (Ahn and Joyner, 2004; Harfe et al., 2004). By contrast, loss of Gli3R or ectopic Shh signaling is detrimental to the anterior skeletal patterning (Li et al., 2014a; Litingtung et al., 2002; Lopez-Rios et al., 2012; Zhang et al., 2010). To determine the relevance of bifunctional Srg3 with respect to skeletal pattern formation, I assessed BMP activity that promotes chondrogenesis at late stages (Karamboulas et al., 2010). In the anterior of *Srg3*$^{f/f}$;*Prx1-cre* forelimb buds, the expression of *Msx2*, which marks the BMP activity (Benazet et al., 2009), was reduced at E10.75 (**Figure 24A,B**) and greatly abolished in the proximal region excluding the distal mesenchyme after ectopic *Shh* was induced (**Figure 24C–F**). By contrast, posterior BMP activity persistently remained low in *Srg3*$^{f/f}$;*Prx1-cre* forelimb buds (**Figure 24A–F**). Among *Bmp* ligands, the expression of both *Bmp2* and *Bmp4*, but not *Bmp7*, was diminished in the posterior mesenchyme of *Srg3*$^{f/f}$;*Prx1-cre* forelimb buds at E11.75 (**Figure 24G–L**). Concurrent downregulation of *Bmp2* and *Bmp4*, which are required for formation of ulna and posterior digits 4 and 5 (Bandyopadhyay et al., 2006), could be causally implicated in the hypoplastic posterior skeletal elements of *Srg3*$^{f/f}$;*Prx1-cre* forelimbs (**Figure 7C,E**). These results indicated that *Srg3* deficiency disrupted BMP activities in the anterior and posterior mesenchyme.

I next examined the distribution of *Sox9*, which marks the condensation of chondrogenic progenitors (Akiyama et al., 2005). *Sox9* expression was remarkably diminished in the primordia giving rise to the scapula prior to E10.75 in *Srg3*$^{f/f}$;*Prx1-*

cre forelimb buds (**Figure 25A,B**). Since the proximal-most skeletal elements might be specified at early limb bud stage (Ahn and Joyner, 2004; Mariani et al., 2008), the reduced AER activity in early *Srg3*-deficient forelimb buds is likely to be a cause of defects in scapula (**Figure 9A**). As limb bud outgrowth distally proceeds, *Sox9*-positive progenitors of *Srg3*$^{f/f}$;*Prx1-cre* forelimb buds were mildly decreased at E11.25 and their subsequent loss was apparently observed in the prospective zeugopod regions at E11.75 (**Figure 25C–F**). In addition, *Sox9*-expressing autopod progenitors in *Srg3*$^{f/f}$;*Prx1-cre* forelimbs did not initiate mesenchymal condensation compared with those in control (**Figure 25E,F**). Consistent with delineation of autopod territories by *Sox9*, *Hoxa13* was detected in the presumptive autopod region of control, whereas it was reduced in the posterior and relatively expanded in the anterior mesenchyme of *Srg3*$^{f/f}$;*Prx1-cre* forelimb buds (**Figure 25G,H**) (Lu et al., 2008). Taken together, *Srg3* deficiency progressively resulted in loss of the *Sox9*-positive progenitors in zeugopod and autopod primordia, which was paralleled by alteration in BMP activities.

To test the effect of ectopic Shh activity on the difference in anterior zeugopod development between *Srg3*$^{f/f}$;*Prx1-cre* forelimbs and hindlimbs, I introduced a single conditional allele of *Twist1* (*Twist1*$^{f/+}$), which represses *Shh* expression in the anterior mesenchyme (Zhang et al., 2010), into the *Srg3*$^{f/f}$;*Prx1-cre* background. *Srg3*$^{f/f}$;*Twist1*$^{f/+}$;*Prx1-cre* hindlimbs exhibited the complete absence of tibia but did not affect the ossification defects and syndactyly of the anterior digits by loss of *Srg3* (n=13/13) (**Figure 26A–D**). Consistently, the reduction of *Sox9*-positive progenitors observed in the tibia primordia of *Srg3*$^{f/f}$;*Twist1*$^{f/+}$;*Prx1-cre* hindlimb buds revealed the correlation with anterior ectopic Shh signaling, which was activated earlier than in *Srg3*$^{f/f}$;*Prx1-cre* hindlimb buds (**Figure 26E–H**). These data suggest that the fate of

anterior skeletal progenitors is progressively determined and the onset timing and dose of ectopic Shh activity are implicated in the severity of anterior zeugopod development.

Bifurcating function of SWI/SNF complex in Hh pathway regulates the spatiotemporal expression of *Grem1*

The low to high transition of BMP activity by the termination of *Grem1* expression is required to initiate condensation and chondrogenic differentiation of proliferative digit progenitors (Bandyopadhyay et al., 2006; Benazet et al., 2009). To gain further insights into the chondrogenic defects in mesenchymal *Srg3*-deficient autopods, the spatial distribution of *Grem1* expression was analyzed at later stages. By E11.75, *Grem1* expression in control forelimb buds began to decline (**Figure 27A**) (Zuniga et al., 2012), but the two domains of *Grem1* in *Srg3*$^{f/f}$;*Prx1-cre* forelimb buds remained separated and these domains had become closer than those of E11.5 (**Figures 23B** and **27B**). At E12.5, *Grem1* expression in control forelimb autopods was cleared from the presumptive digit territories and confined to the interdigital mesenchyme (**Figure 27C**), whereas in *Srg3*$^{f/f}$;*Prx1-cre* forelimb autopods, the split domains of *Grem1* were joined into the one continuous domain with upregulated expression in the anterior autopods (**Figure 27D**). At this stage, the upregulation of *Msx2* expression was not observed in the interdigital mesenchyme of *Srg3*$^{f/f}$;*Prx1-cre* forelimb autopods compared to control (**Figure 27E,F**). The increased *Grem1* expression and low BMP activity were also remarkably observed in the anterior autopods of *Srg3*-deficient hindlimbs (**Figure 27G,F**). These data suggested that low Shh response in *Srg3*-

deficient forelimb buds delayed the propagation of *Grem1* and subsequently disturbed the progression from low to high BMP signaling in the anterior and interdigital mesenchyme.

I next examined whether the prolonged distribution of *Grem1* is correlated with chondrogenesis of digit primordia. The delayed mesenchymal condensations revealed by distribution of *Sox9* in autopod primordia were definitely observed in *Srg3*$^{f/f}$;*Prx1-cre* limbs (**Figures 25E,F** and **28A,B,E–H**). Furthermore, the mesenchymal condensations of five digit primordia were apparent in control autopods (**Figure 28A,G**), whereas condensations of anterior digit progenitors were relatively less induced than those of posterior ones in *Srg3*-deficient autopods (**Figure 28B,H**). This delay was corroborated by activation of *Col2a1* transcript marking chondrogenic differentiation as a target gene of Sox9 (Bell et al., 1997). In *Srg3*-deficient autopods, *Col2a1* was expressed in the primordia corresponding to digits 3 to 5 of control forelimbs and digits 2 to 5 of control hindlimbs and was conversely absent in the anterior mesenchyme (**Figure 28C,D,I,J**). Thus, the comparison of *Col2a1* transcript distributions in *Srg3*-deficient forelimb and hindlimb autopods revealed that both the extent of *Grem1* propagation and its anterior upregulation caused the sequential onset of chondrogenesis in the posterior and anterior autopods.

As the low to high transition of BMP activity is not timely regulated, cell death of mesenchymal digit progenitors or interdigital apoptosis abnormally occurs (Bandyopadhyay et al., 2006; Farin et al., 2013; Lopez-Rios et al., 2012; Pajni-Underwood et al., 2007). Thus, I examined whether the delayed propagation and anterior upregulation of *Grem1* expression affects the distribution of apoptotic cells. In E12.5 *Srg3*$^{f/f}$;*Prx1-cre* forelimb autopods, Lysotracker Red staining showed the increase of apoptotic cells in the distal mesenchyme underlying the AER, particularly

in the combined regions of *Grem1* domains (**Figure 29A,B**). Low Grem1 activity by its delay in this region likely causes the transient elevation of BMP signaling, resulting in cell death prior to the onset of chondrogenesis. Furthermore, the reduction of interdigital apoptosis, resulting in soft tissue syndactyly, was observed in the anterior autopods of *Srg3*$^{f/f}$;*Prx1-cre* forelimbs at E13.5 and hindlimbs at E12.5 (**Figure 29C,D,G,H**). Consistent with this, the enhanced expression of *Fgf8*, which is required for the shutdown of *Grem1* expression (Verheyden and Sun, 2008), was confirmed in *Srg3*$^{f/f}$;*Prx1-cre* anterior autopods (**Figure 29E,F,I,J**). Taken together, these data revealed that the spatiotemporal regulation of *Grem1* expression and its BMP antagonism are required for cell survival during expansion of autopod progenitors and for inducing apoptosis in the interdigital mesenchyme. Thus, SWI/SNF complex is involved in the late determinative processes influenced by Grem1-mediated BMP antagonism through bifurcating action in Hh pathway.

Figure 24. Disrupted BMP signaling in *Srg3*-deficient forelimb buds

(**A**–**F**) Spatiotemporal distribution of *Msx2* transcripts in control and *Srg3*$^{f/f}$;*Prx1-cre* forelimb buds at indicated stages. Red and Black arrowheads indicate the anterior and posterior domains, respectively.

(**G**–**L**) Expression of *Bmp2*, *Bmp4* and *Bmp7* in control and *Srg3*$^{f/f}$;*Prx1-cre* forelimb buds at E11.75. Black arrowheads denote posterior expression domains.

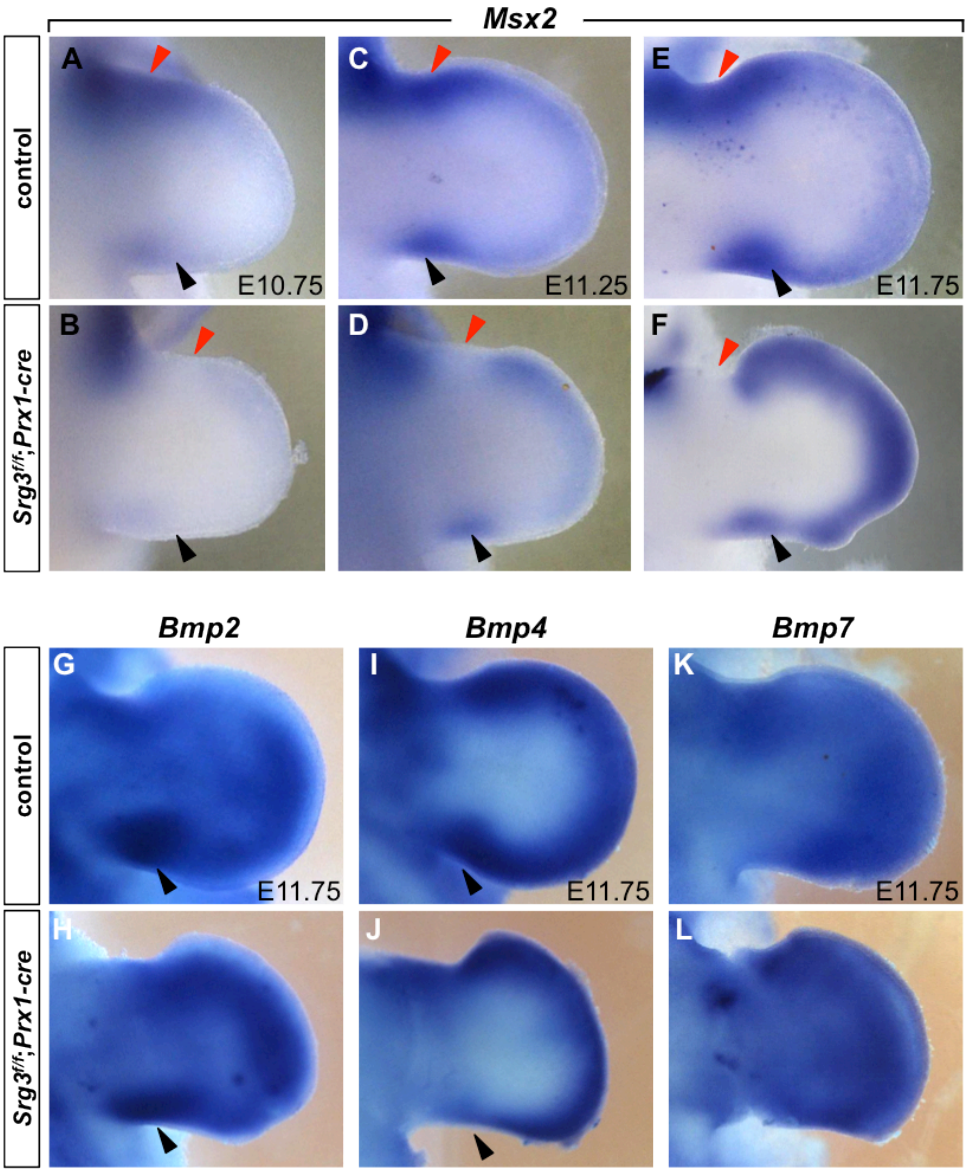
Msx2
control
Srg3f/f;Prx1-cre
A
B
C
D
E
F
E10.75
E11.25
E11.75
Bmp2
Bmp4
Bmp7
G
H
I
J
K
L
E11.75
E11.75
E11.75

Figure 25. Defective chondrogenic differentiation in *Srg3*-deficient forelimb buds

(**A**–**F**) Distribution of *Sox9* in control and *Srg3*$^{f/f}$;*Prx1-cre* forelimb buds at indicated stages. Red and black arrowheads indicate the primordia corresponding to scapula and zeugopod, respectively. Brackets show the width of presumptive autopod region. The following abbreviations are used for primordia: a, autopod; h, humerus; r, radius; sc, scapula; u, ulna; asterisks, digit rays.

(**G**,**H**) Expression of *Hoxa13* in E11.75 control and *Srg3*$^{f/f}$;*Prx1-cre* forelimb buds. Red and black arrowheads point to the anterior expansion and posterior decrease in *Srg3*$^{f/f}$;*Prx1-cre* forelimb bud, respectively.

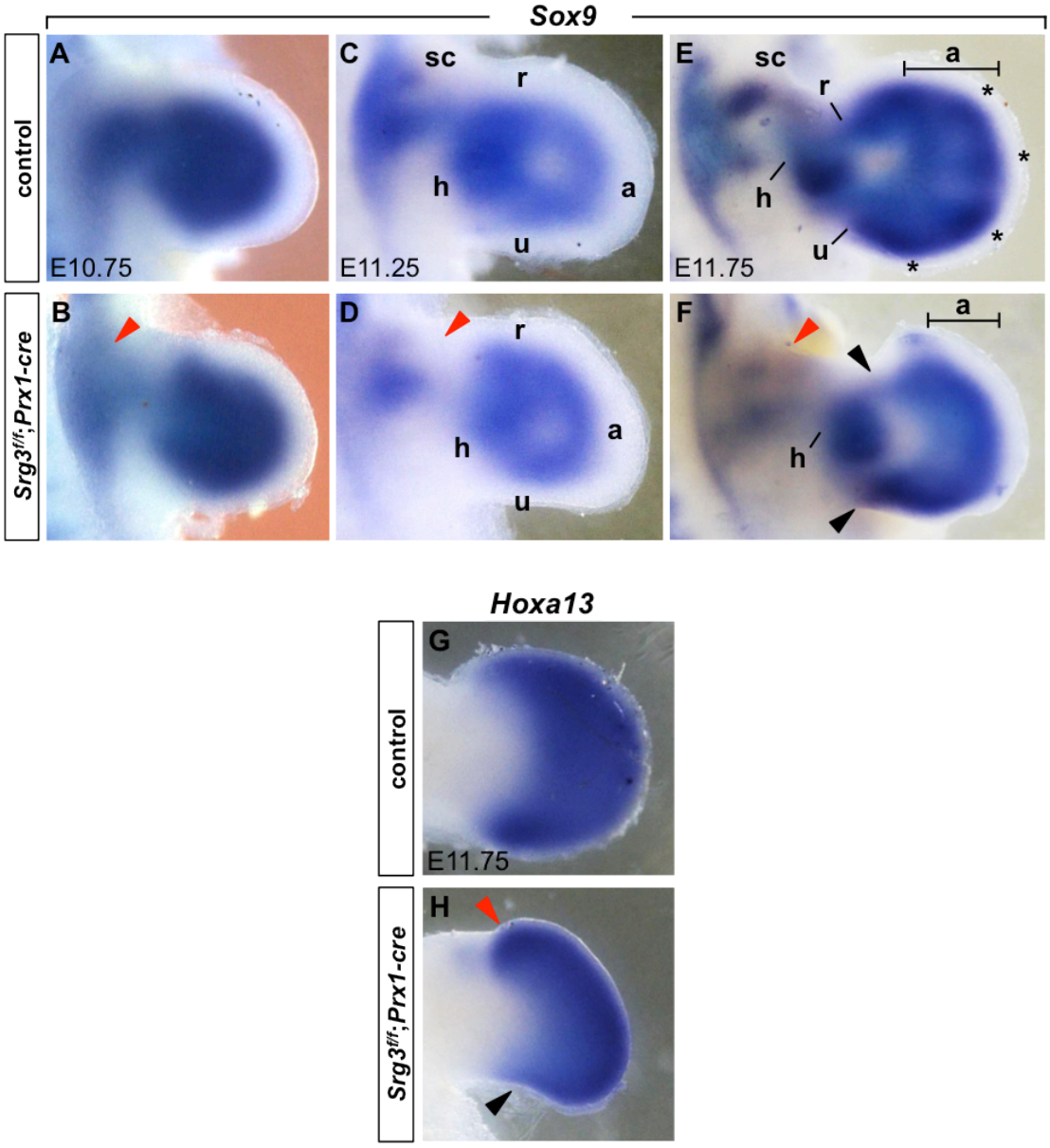
Sox9
control
Srg3f/f;Prx1-cre
A
B
C
D
E
F
G
H
sc
r
h
a
u
E10.75
E11.25
E11.75
Hoxa13

Figure 26. Genetic interaction between *Srg3* and *Twist1* in hindlimb development.

(**A**–**D**) Skeletal preparations from *Twist1*$^{f/+}$;*Prx1-cre* and *Srg3*$^{f/f}$;*Twist1*$^{f/+}$;*Prx1-cre* hindlimbs at P0. Red arrowhead in (**B**) indicates loss of tibia. Black arrowheads in (**D**) indicate ossification defects and syndactyly in anterior digits. Abbreviations: fe, femur; fi, fibula; pg, pelvic girdle; ti, tibia.

(**E**–**H**) Distribution of *Sox9* and *Gli1* in *Twist1*$^{f/+}$;*Prx1-cre* and *Srg3*$^{f/f}$;*Twist1*$^{f/+}$;*Prx1-cre* hindlimbs at indicated stages.

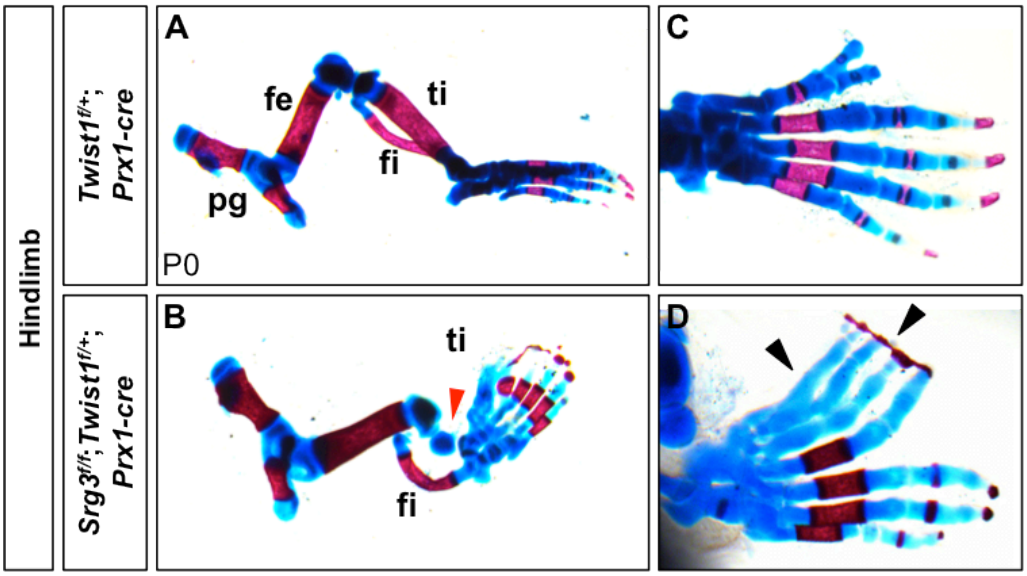
Hindlimb
Twist1f/+; Prx1-cre
Srg3f/f; Twist1f/+; Prx1-cre
A
fe
ti
fi
pg
P0
B
ti
fi
C
D

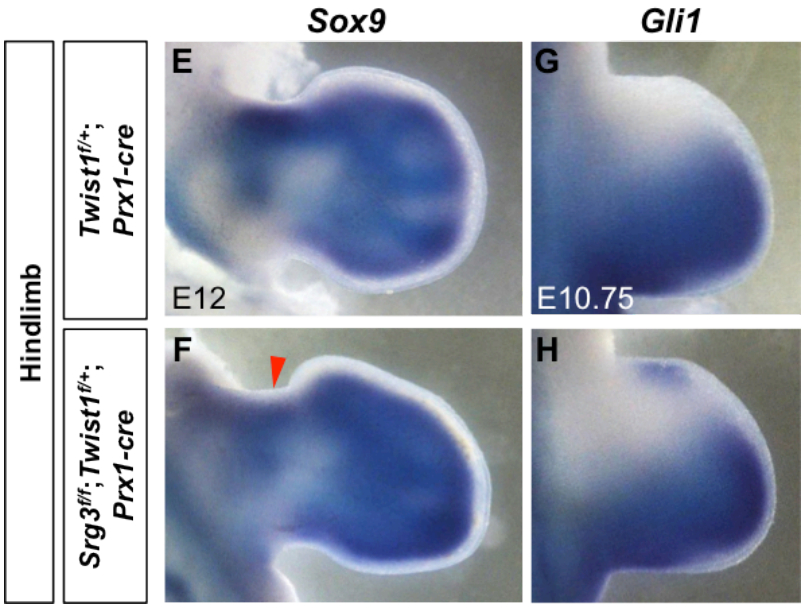
Sox9
Gli1
Hindlimb
Twist1f/+; Prx1-cre
Srg3f/f; Twist1f/+; Prx1-cre
E
E12
G
E10.75
F
H

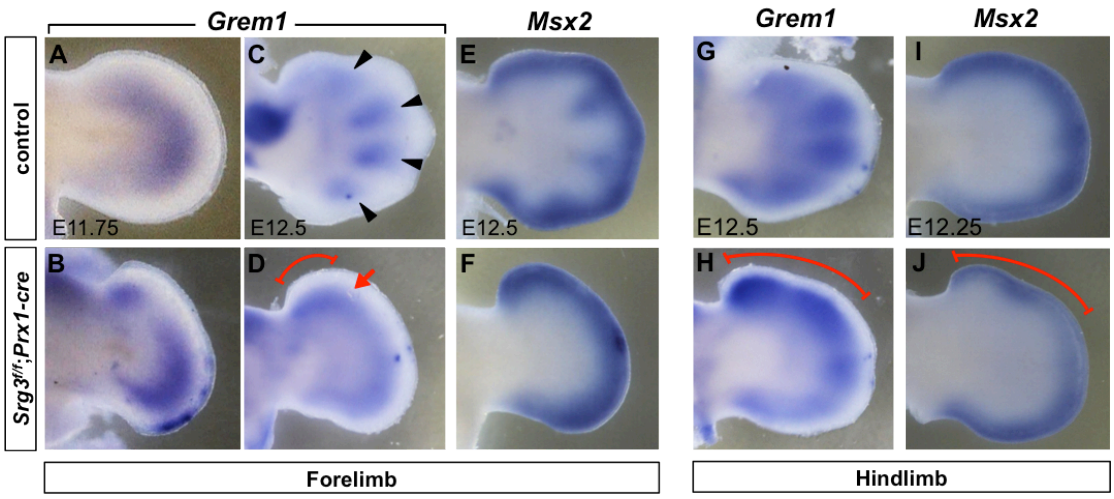

Figure 27. Delayed *Grem1* expression retards the low to high transition of BMP activity in *Srg3*-deficient limb buds.

(**A**–**J**) Distribution of *Grem1* and *Msx2* transcripts in control and *Srg3*$^{f/f}$;*Prx1-cre* forelimb and hindlimb autopods at indicated stages. The spatial restriction to the interdigital mesenchyme (arrowheads in **C**), combined region of separate domains (arrow in **D**), enhanced region (brackets in **D** and **H**) of *Grem1* and reduced BMP activity (bracket in **J**) are indicated.

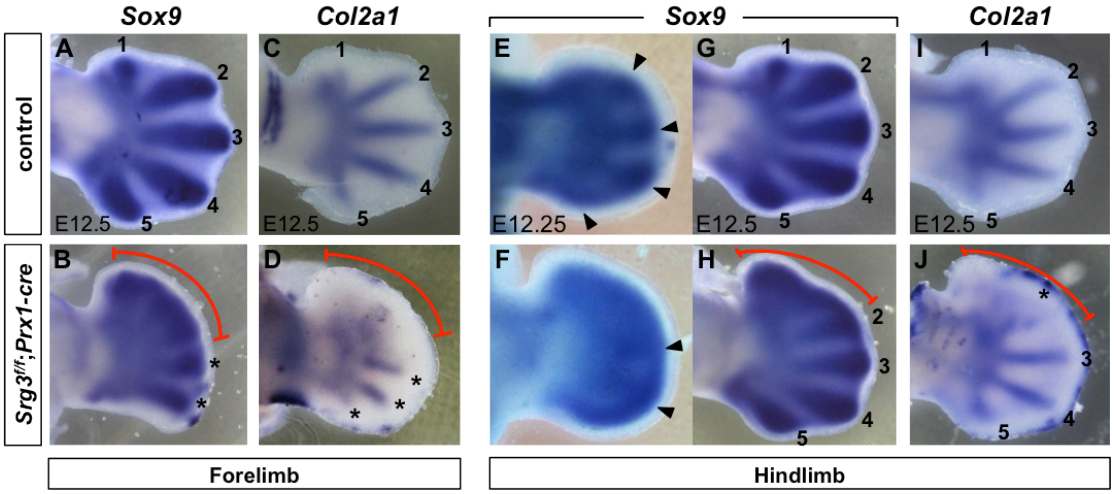

Figure 28. Delayed *Grem1*–mediated BMP antagonism causes the sequential onset of chondrogenesis in the posterior and anterior autopods lacking *Srg3*.

(**A**–**J**) Expression of *Sox9* and *Col2a1* in E12.5 control and *Srg3*$^{f/f}$;*Prx1-cre* forelimb and hindlimb autopods. Brackets indicate the delayed region of chondrogenic differentiation. Numbers 1 to 5 indicate primordia of digit rays 1 to 5. Asterisks in (**B** and **D**) indicate the preceding chondrogenesis of shortened digit primordia in the posterior.

Figure 29. Srg3-mediated regulation of *Grem1* expression affects the expansion of limb progenitors and the interdigital programmed cell death.

(**A**–**J**) Distribution of apoptotic cells by Lysotracker Red staining and *Fgf8* transcripts in control and *Srg3*$^{f/f}$;*Prx1-cre* forelimb and hindlimb autopods at indicated stages. Arrow in (**B**) points to the increased cell death. White dotted lines in (**D** and **H**) indicated the absence of interdigital mesenchymal cell death. Brackets in (**F** and **J**) denote the upregulated *Fgf8* expression.

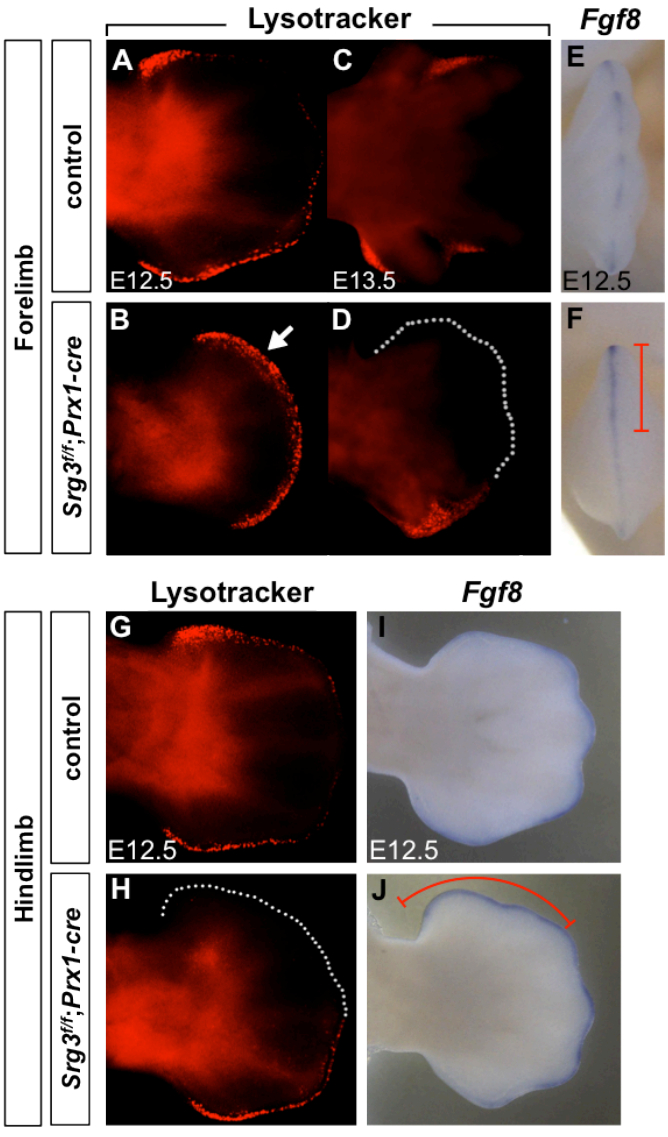
Lysotracker
Fgf8
Forelimb
control
Srg3f/f;Prx1-cre
A
C
E
B
D
F
E12.5
E13.5
E12.5
Lysotracker
Fgf8
Hindlimb
control
Srg3f/f;Prx1-cre
G
I
H
J
E12.5
E12.5

IV. Discussion

In this study, I uncovered the dual requirement of SWI/SNF complex in Hh pathway during limb AP skeletal patterning. The genetic and molecular analyses of *Srg3* have shown that SWI/SNF complex is required for modulating the response to Shh and repressing anterior ectopic Hh pathway. Recent studies have identified the gene networks of *trans*-acting regulators by interacting with multiple *cis*-regulatory modules (CRM) in the genomic landscapes of transcription factors orchestrating limb development (Li et al., 2014b; Osterwalder et al., 2014; Vokes et al., 2008). Phenotypes observed in constitutive or conditional loss-of-function mutants might reflect various outputs of these regulatory networks from early limb bud stages onward. By contrast, genetic analysis of mesenchymal *Srg3* helps me to describe the molecular mechanism that integrates the transcriptional regulation of Hh signaling by SWI/SNF chromatin remodeling complex with Grem1-BMP antagonism without severe defects in the formation of signaling centers.

Importantly, this study provides insights into how SWI/SNF complex contributes to the transcriptional programs in mesenchymal cells responding to diffusible morphogen activity. In the posterior of *Srg3*-deficient forelimb buds, the coincident failure to anteriorly expand the expression of both *Gli1* and *Ptch1* indicates a deficiency in long-range effects of Shh. This is consistent with the idea that a gradient of *Ptch1* expression is required for graded Shh activity established by dose and exposed duration of signal (Dessaud et al., 2007; Harfe et al., 2004). Loss of Ptch1 in the developing limb is accompanied by concurrent activation of Hh pathway (Butterfield et al., 2009; Zhulyn et al., 2014), since Ptch1-mediated sequestration of Shh is required to properly restrain Shh diffusion (Briscoe et al., 2001; Chen and Struhl, 1996). By contrast, mesenchymal *Srg3* deficiency allows Hh pathway to be activated within the ectoderm beyond the range of *Prx1-cre* activity and its underlying

distal-most mesenchyme. The molecular alterations between *Srg3*-deficient and *Ptch1*-deficient forelimb buds are similar except the *Gli1* expression. The alterations appear to be the effects of low Shh sensing corroborated by the distalization of epithelial-mesenchymal signaling and *Hoxd13*-positive presumptive autopod region (Lopez-Rios et al., 2014). Owing to the reduced mesenchymal responses to Shh, *Srg3*$^{f/f}$;*Prx1-cre* forelimb buds seem to progress further than *Ptch1*-deficient forelimb buds in the chondrogenic differentiation of the zeugopod and autopod primordia (Bruce et al., 2010). Therefore, my skeletal analysis reveals that the formation of ulna and digits 2-5 directed by graded Shh signaling is achieved through modulation of Shh responsiveness by SWI/SNF complex (Ahn and Joyner, 2004; Harfe et al., 2004). Based on these findings, I suggest that SWI/SNF complex regulates cellular responses to Shh by modulating both the sensing and downstream transduction of signals.

Intriguingly, conditional inactivation of *Srg3* in the limb bud mesenchyme induces ectopic and anteriorized *Shh* expression. Previous studies have suggested the autoregulatory mechanisms ensuring the proper amount of Shh in the mesenchyme and AER of posterior limb bud to accomplish the distal limb patterning (Bouldin et al., 2010; Sanz-Ezquerro and Tickle, 2000). The failure to constrain *Shh* expression to the posterior margin in *Srg3*$^{f/f}$;*Prx1-cre* limb buds might be caused by the decreased cellular response to Shh in the core mesenchyme. I cannot rule out the possibility that SWI/SNF complex directly represses the expression of *Shh* through the regulation of limb-specific *Shh* enhancer ZRS (ZPA regulatory sequence) (Lettice et al., 2003) or other pathways. In this context, however, as the ZRS has no Gli-binding sites (Galli et al., 2010; Vokes et al., 2008), Gli-SWI/SNF complex is unlikely to be involved in regulating ZRS. Rather, the absence of long-range Shh signaling or the ligand binding capacity of ectopic Ptch1 presumably enables the redistribution of *Shh*-expressing

cells and their descendants in *Srg3*$^{f/f}$;*Prx1-cre* limb buds.

With respect to the anterior mesenchyme, this study provides the evidence for dissecting the functions of GliR, mainly Gli3R. *Srg3* deficiency establishes intact AP polarity in early limb buds but recapitulates the molecular alterations of limb buds constitutively lacking *Gli3* in the anterior mesenchyme at E10.5 (Galli et al., 2010; Litingtung et al., 2002; te Welscher et al., 2002b). However, analysis of *Msx2* distribution in *Srg3*$^{f/f}$;*Prx1-cre* forelimb buds shows distinct BMP activities in the zeugopod and autopod primordia of anterior mesenchyme over time, unlike its reduction throughout the anterior mesenchyme in *Gli3*-deficient limb buds (Lopez-Rios et al., 2012). The comparison of anterior zeugopod development and digit numbers between *Srg3*$^{f/f}$;*Prx1-cre* forelimbs and hindlimbs reveals that the dose and exposed duration of ectopic Shh activity negatively impact the differentiation of anterior prechondrogenic progenitors. Together with these findings, previous observations have demonstrated that the expansion of Hh signaling has an inhibitory effect on the formation of anterior skeletal elements (Li et al., 2014a; Litingtung et al., 2002; Zhang et al., 2010; Zhulyn et al., 2014). The detrimental effect of Shh activity on digit 1 appears to be dependent on the timing it reaches the anterior-most progenitor population. In this regard, the proliferative expansion of anterior progenitors negatively controlled by Gli3 might require the time to ensure a sufficient population such as both *Irx3*- and *Irx5*-positive early progenitors (Li et al., 2014a; Lopez-Rios et al., 2012). In addition, the regional effects of Shh activity at late stages could alter the morphogenic gradient and result in the expansion of anterior autopod progenitors by low Gli3R. Therefore, the fate of anterior mesenchymal progenitors governed by GliR activity is flexible to external stimuli and progressively determined throughout the proximodistal mesenchyme.

This study highlights the sustained requirement of Shh responsiveness for regulating Grem1 activity previously undetected due to its severe loss in *Shh*$^{-/-}$ mutants or its symmetric expansion in both *Gli3*$^{-/-}$ and *Shh*$^{-/-}$;*Gli3*$^{-/-}$ mutants (Litingtung et al., 2002; Panman et al., 2006; te Welscher et al., 2002b). The anterior redistribution and delayed propagation of *Grem1* expression in *Srg3*$^{f/f}$;*Prx1-cre* forelimb buds resulted in dissociation of its domains, which clarified that the propagation of *Grem1* requires the SWI/SNF complex-mediated modulation of Shh responsiveness. It has recently been suggested that limb-specific enhancers integrated by posterior GliA- and anterior GliR-dependent CRMs regulate the transcriptional activity of *Grem1* (Li et al., 2014b). Consistently, the dynamic redistribution of *Grem1* in *Srg3*$^{f/f}$;*Prx1-cre* forelimb buds could be a consequence of reconstitution of GliA/GliR gradient by ectopic Shh activity and low Shh response. Furthermore, the propagation of *Grem1* by Shh responsiveness affects anterior skeletal formation, particularly digit 2 primordium, together with restriction and termination of *Grem1* by Gli3 (Lopez-Rios et al., 2012). Thus, the bifunctional roles of SWI/SNF complex in Hh pathway mediate AP skeletal patterning elicited by GliA and GliR functions through the spatiotemporal regulation of *Grem1* (Bowers et al., 2012; Lopez-Rios et al., 2012; this study).

The interaction of Srg3-containing SWI/SNF complex with bifunctional Gli proteins might involve the recruitment of histone modifying enzymes to regulatory regions of Hh target genes (Canettieri et al., 2010; Cheng and Bishop, 2002; Zhan et al., 2011). A recent study has also shown that SWI/SNF complex can control chromatin structure through functional cooperation with cofactors (Choi et al., 2015). Nonetheless, since it was reported that ATPase Brg1 regulates Hh target genes in an ATPase-independent manner during neural development (Zhan et al., 2011), the distinct changes in histone

modifications between anterior and posterior limb skeletal progenitors lacking *Srg3* remain to be elucidated.

I have demonstrated that SWI/SNF complex plays an integral role conferring the graded signaling upon limb bud mesenchymal cells responding to Shh (**Figure 30**). SWI/SNF complex influences the progression of interlinked morphogen signaling pathways by modulating Shh responsiveness in the posterior mesenchyme and also by repressing Hh pathway in Shh-free region. This study showing the effects of epigenetic regulation by SWI/SNF chromatin remodeling complex on limb patterning provides new insights into deciphering morphogen gradients.

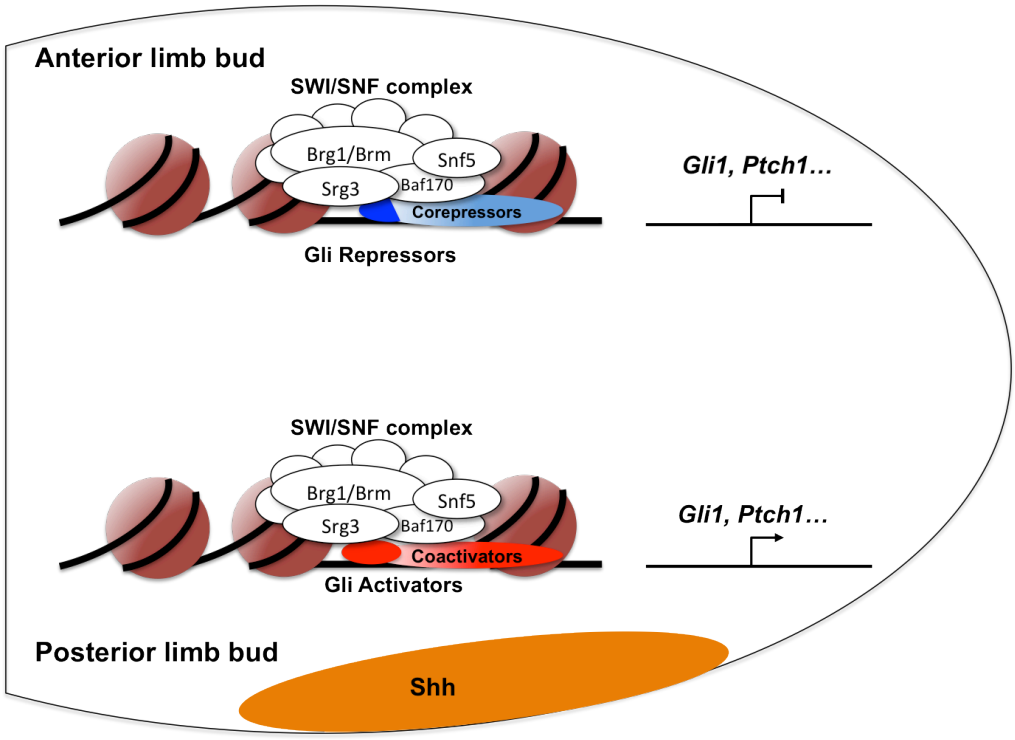

Figure 30. A possible model for the role of SWI/SNF chromatin remodeling complex in Hedgehog pathway during limb development.

The gradient of GliA and GliR is generated by graded Shh signaling along AP axis of limb bud. GliA and GliR interacts with Srg3-containing SWI/SNF chromatin remodeling complex in a gradient-dependent manner and these Gli-SWI/SNF complexes alter the chromatin status with histone modifying enzymes to activate or repress the Shh/Gli target genes.

V. References

Ahn, S., and Joyner, A.L. (2004). Dynamic changes in the response of cells to positive hedgehog signaling during mouse limb patterning. *Cell* 118, 505-516.

Akiyama, H., Kim, J.E., Nakashima, K., Balmes, G., Iwai, N., Deng, J.M., Zhang, Z., Martin, J.F., Behringer, R.R., Nakamura, T., *et al*. (2005). Osteo-chondroprogenitor cells are derived from Sox9 expressing precursors. *Proc Natl Acad Sci* 102, 14665-14670.

Anderson, E., Devenney, P.S., Hill, R.E., and Lettice, L.A. (2014). Mapping the Shh long-range regulatory domain. *Development* 141, 3934-3943.

Bai, C.B., Stephen, D., and Joyner, A.L. (2004). All mouse ventral spinal cord patterning by hedgehog is Gli dependent and involves an activator function of Gli3. *Dev Cell* 6, 103-115.

Bandyopadhyay, A., Tsuji, K., Cox, K., Harfe, B.D., Rosen, V., and Tabin, C.J. (2006). Genetic analysis of the roles of BMP2, BMP4, and BMP7 in limb patterning and skeletogenesis. *PLoS Genet* 2, e216.

Barnfield, P.C., Zhang, X., Thanabalasingham, V., Yoshida, M., and Hui, C.C. (2005). Negative regulation of Gli1 and Gli2 activator function by Suppressor of fused through multiple mechanisms. *Differentiation* 73, 397-405.

Barrow, J.R., Thomas, K.R., Boussadia-Zahui, O., Moore, R., Kemler, R., Capecchi, M.R., and McMahon, A.P. (2003). Ectodermal Wnt3/beta-catenin signaling is required for the establishment and maintenance of the apical ectodermal ridge. *Genes Dev* 17, 394-409.

Belandia, B., Orford, R.L., Hurst, H.C., and Parker, M.G. (2002). Targeting of SWI/SNF chromatin remodelling complexes to estrogen-responsive genes. *EMBO J* 21, 4094-4103.

Bell, D.M., Leung, K.K., Wheatley, S.C., Ng, L.J., Zhou, S., Ling, K.W., Sham, M.H., Koopman, P., Tam, P.P., and Cheah, K.S. (1997). SOX9 directly regulates the type-II collagen gene. *Nat Genet* 16, 174-178.

Bell, S.M., Schreiner, C.M., Goetz, J.A., Robbins, D.J., and Scott, W.J., Jr. (2005). Shh signaling in limb bud ectoderm: potential role in teratogen-induced postaxial ectrodactyly. *Dev Dyn* 233, 313-325.

Benazet, J.D., Bischofberger, M., Tiecke, E., Goncalves, A., Martin, J.F., Zuniga, A., Naef, F., and Zeller, R. (2009). A self-regulatory system of interlinked signaling feedback loops controls mouse limb patterning. *Science* 323, 1050-1053.

Borrelli, E., Nestler, E.J., Allis, C.D., and Sassone-Corsi, P. (2008). Decoding the epigenetic language of neuronal plasticity. *Neuron* 60, 961-974.

Bouldin, C.M., Gritli-Linde, A., Ahn, S., and Harfe, B.D. (2010). Shh pathway activation is present and required within the vertebrate limb bud apical ectodermal ridge for normal autopod patterning. *Proc Natl Acad Sci* 107, 5489-5494.

Bowers, M., Eng, L., Lao, Z., Turnbull, R.K., Bao, X., Riedel, E., Mackem, S., and Joyner, A.L. (2012). Limb anterior-posterior polarity integrates activator and repressor functions of GLI2 as well as GLI3. *Dev Biol* 370, 110-124.

Briscoe, J., Chen, Y., Jessell, T.M., and Struhl, G. (2001). A hedgehog-insensitive form of patched provides evidence for direct long-range morphogen activity of sonic hedgehog in the neural tube. *Mol Cell* 7, 1279-1291.

Briscoe, J., and Therond, P.P. (2013). The mechanisms of Hedgehog signalling and its roles in development and disease. *Nat Rev Mol Cell Biol* 14, 416-429.

Bruce, S.J., Butterfield, N.C., Metzis, V., Town, L., McGlinn, E., and Wicking, C. (2010). Inactivation of Patched1 in the mouse limb has novel inhibitory effects on the chondrogenic program. *J Biol Chem* 285, 27967-27981.

Bultman, S., Gebuhr, T., Yee, D., La Mantia, C., Nicholson, J., Gilliam, A., Randazzo, F., Metzger, D., Chambon, P., Crabtree, G., *et al*. (2000). A Brg1 null mutation in the mouse reveals functional differences among mammalian SWI/SNF complexes. *Mol Cell* 6, 1287-1295.

Buscher, D., Bosse, B., Heymer, J., and Ruther, U. (1997). Evidence for genetic control of Sonic hedgehog by Gli3 in mouse limb development. *Mech Dev* 62, 175-182.

Butterfield, N.C., Metzis, V., McGlinn, E., Bruce, S.J., Wainwright, B.J., and Wicking, C. (2009). Patched 1 is a crucial determinant of asymmetry and digit number in the vertebrate limb. *Development* 136, 3515-3524.

Cairns, B.R., Kim, Y.J., Sayre, M.H., Laurent, B.C., and Kornberg, R.D. (1994). A multisubunit complex containing the SWI1/ADR6, SWI2/SNF2, SWI3, SNF5, and SNF6 gene products isolated from yeast. *Proc Natl Acad Sci* 91, 1950-1954.

Canettieri, G., Di Marcotullio, L., Greco, A., Coni, S., Antonucci, L., Infante, P., Pietrosanti, L., De Smaele, E., Ferretti, E., Miele, E., *et al*. (2010). Histone deacetylase and Cullin3-REN(KCTD11) ubiquitin ligase interplay regulates Hedgehog signalling through Gli acetylation. *Nat Cell Biol* 12, 132-142.

Cao, T., Wang, C., Yang, M., Wu, C., and Wang, B. (2013). Mouse limbs expressing only the Gli3 repressor resemble those of Sonic hedgehog mutants. *Dev Biol* 379, 221-228.

Capellini, T.D., Di Giacomo, G., Salsi, V., Brendolan, A., Ferretti, E., Srivastava, D., Zappavigna, V., and Selleri, L. (2006). Pbx1/Pbx2 requirement for distal limb patterning is mediated by the hierarchical control of Hox gene spatial distribution and Shh expression. *Development* 133, 2263-2273.

Chen, J., and Archer, T.K. (2005). Regulating SWI/SNF subunit levels via protein-protein interactions and proteasomal degradation: BAF155 and BAF170 limit expression of BAF57. *Mol Cell Biol* 25, 9016-9027.

Chen, J.K., Taipale, J., Cooper, M.K., and Beachy, P.A. (2002). Inhibition of Hedgehog signaling by direct binding of cyclopamine to Smoothened. *Genes Dev* 16, 2743-2748.

Chen, Y., and Struhl, G. (1996). Dual roles for patched in sequestering and transducing Hedgehog. *Cell* 87, 553-563.

Cheng, S.W., Davies, K.P., Yung, E., Beltran, R.J., Yu, J., and Kalpana, G.V. (1999). c-MYC interacts with INI1/hSNF5 and requires the SWI/SNF complex for transactivation function. *Nat Genet* 22, 102-105.

Cheng, S.Y., and Bishop, J.M. (2002). Suppressor of Fused represses Gli-mediated transcription by recruiting the SAP18-mSin3 corepressor complex. *Proc Natl Acad Sci* 99, 5442-5447.

Chi, T.H., Wan, M., Zhao, K., Taniuchi, I., Chen, L., Littman, D.R., and Crabtree, G.R. (2002). Reciprocal regulation of CD4/CD8 expression by SWI/SNF-like BAF complexes. *Nature* 418, 195-199.

Chiang, C., Litingtung, Y., Harris, M.P., Simandl, B.K., Li, Y., Beachy, P.A., and Fallon, J.F. (2001). Manifestation of the limb prepattern: limb development in the absence of sonic hedgehog function. *Dev Biol* 236, 421-435.

Choi, J., Ko, M., Jeon, S., Jeon, Y., Park, K., Lee, C., Lee, H., and Seong, R.H. (2012). The SWI/SNF-like BAF complex is essential for early B cell development. *J Immunol* 188, 3791-3803.

Choi, J., Jeon, S., Choi, S., Park, K., and Seong, R.H. (2015). The SWI/SNF chromatin remodeling complex regulates germinal center formation by repressing Blimp-1 expression. *Proc Natl Acad Sci* 112, E718-727.

Collins, R.T., Furukawa, T., Tanese, N., and Treisman, J.E. (1999). Osa associates with the Brahma chromatin remodeling complex and promotes the activation of some target genes. *EMBO J* 18, 7029-7040.

Crossley, P.H., and Martin, G.R. (1995). The mouse Fgf8 gene encodes a family of polypeptides and is expressed in regions that direct outgrowth and patterning in the developing embryo. *Development* 121, 439-451.

Dahn, R.D., and Fallon, J.F. (2000). Interdigital regulation of digit identity and homeotic transformation by modulated BMP signaling. *Science* 289, 438-441.

Dai, P., Akimaru, H., Tanaka, Y., Maekawa, T., Nakafuku, M., and Ishii, S. (1999). Sonic Hedgehog-induced activation of the Gli1 promoter is mediated by GLI3. *J Biol Chem* 274, 8143-8152.

Dessaud, E., Yang, L.L., Hill, K., Cox, B., Ulloa, F., Ribeiro, A., Mynett, A., Novitch, B.G., and Briscoe, J. (2007). Interpretation of the sonic hedgehog morphogen gradient by a temporal adaptation mechanism. *Nature* 450, 717-720.

Dingwall, A.K., Beek, S.J., McCallum, C.M., Tamkun, J.W., Kalpana, G.V., Goff, S.P., and Scott, M.P. (1995). The Drosophila snr1 and brm proteins are related to yeast SWI/SNF proteins and are components of a large protein complex. *Mol Biol Cell* 6, 777-791.

Farin, H.F., Ludtke, T.H., Schmidt, M.K., Placzko, S., Schuster-Gossler, K., Petry, M., Christoffels, V.M., and Kispert, A. (2013). Tbx2 terminates shh/fgf signaling in the developing mouse limb bud by direct repression of gremlin1. *PLoS Genet* 9, e1003467.

Galli, A., Robay, D., Osterwalder, M., Bao, X., Benazet, J.D., Tariq, M., Paro, R., Mackem, S., and Zeller, R. (2010). Distinct roles of Hand2 in initiating polarity and posterior Shh expression during the onset of mouse limb bud development. *PLoS Genet* 6, e1000901.

Guidi, C.J., Sands, A.T., Zambrowicz, B.P., Turner, T.K., Demers, D.A., Webster, W., Smith, T.W., Imbalzano, A.N., and Jones, S.N. (2001). Disruption of Ini1 leads to peri-implantation lethality and tumorigenesis in mice. *Mol Cell Biol* 21, 3598-3603.

Han, D., Jeon, S., Sohn, D.H., Lee, C., Ahn, S., Kim, W.K., Chung, H., and Seong, R.H. (2008). SRG3, a core component of mouse SWI/SNF complex, is essential for extra-embryonic vascular development. *Dev Biol* 315, 136-146.

Harfe, B.D., Scherz, P.J., Nissim, S., Tian, H., McMahon, A.P., and Tabin, C.J. (2004). Evidence for an expansion-based temporal Shh gradient in specifying vertebrate digit identities. *Cell* 118, 517-528.

Hargreaves, D.C., and Crabtree, G.R. (2011). ATP-dependent chromatin remodeling: genetics, genomics and mechanisms. *Cell Res* 21, 396-420.

Harikrishnan, K.N., Chow, M.Z., Baker, E.K., Pal, S., Bassal, S., Brasacchio, D., Wang, L., Craig, J.M., Jones, P.L., Sif, S., *et al*. (2005). Brahma links the SWI/SNF chromatin-remodeling complex with MeCP2-dependent transcriptional silencing. *Nat Genet* 37, 254-264.

Hassan, A.H., Prochasson, P., Neely, K.E., Galasinski, S.C., Chandy, M., Carrozza, M.J., and Workman, J.L. (2002). Function and selectivity of bromodomains in anchoring chromatin-modifying complexes to promoter nucleosomes. *Cell* 111, 369-379.

Hebert, J.M., Basilico, C., Goldfarb, M., Haub, O., and Martin, G.R. (1990). Isolation of cDNAs encoding four mouse FGF family members and characterization of their expression patterns during embryogenesis. *Dev Biol* 138, 454-463.

Hill, P., Wang, B., and Ruther, U. (2007). The molecular basis of Pallister Hall associated polydactyly. *Hum Mol Genet* 16, 2089-2096.

Hill, P., Gotz, K., and Ruther, U. (2009). A SHH-independent regulation of Gli3 is a significant determinant of anteroposterior patterning of the limb bud. *Dev Biol* 328, 506-516.

Hirabayashi, Y., and Gotoh, Y. (2010). Epigenetic control of neural precursor cell fate during development. *Nat Rev Neurosci* 11, 377-388.

Ho, L., Jothi, R., Ronan, J.L., Cui, K., Zhao, K., and Crabtree, G.R. (2009a). An embryonic stem cell chromatin remodeling complex, esBAF, is an essential component of the core pluripotency transcriptional network. *Proc Natl Acad Sci* 106, 5187-5191.

Ho, L., Ronan, J.L., Wu, J., Staahl, B.T., Chen, L., Kuo, A., Lessard, J., Nesvizhskii, A.I., Ranish, J., and Crabtree, G.R. (2009b). An embryonic stem cell chromatin remodeling complex, esBAF, is essential for embryonic stem cell self-renewal and pluripotency. *Proc Natl Acad Sci* 106, 5181-5186.

Ho, L., and Crabtree, G.R. (2010). Chromatin remodelling during development. *Nature* 463, 474-484.

Hui, C.C., and Joyner, A.L. (1993). A mouse model of greig cephalopolysyndactyly syndrome: the extra-toesJ mutation contains an intragenic deletion of the Gli3 gene. *Nat Genet* 3, 241-246.

Hui, C.C., and Angers, S. (2011). Gli proteins in development and disease. *Annu Rev Cell Dev Biol* 27, 513-537.

Ingham, P.W., and McMahon, A.P. (2001). Hedgehog signaling in animal development: paradigms and principles. *Genes Dev* 15, 3059-3087.

Jacob, J., and Briscoe, J. (2003). Gli proteins and the control of spinal-cord patterning. *EMBO Rep* 4, 761-765.

Jagani, Z., Mora-Blanco, E.L., Sansam, C.G., McKenna, E.S., Wilson, B., Chen, D., Klekota, J., Tamayo, P., Nguyen, P.T., Tolstorukov, M.*, et al*. (2010). Loss of the tumor suppressor Snf5 leads to aberrant activation of the Hedgehog-Gli pathway. *Nat Med* 16, 1429-1433.

Jessell, T.M. (2000). Neuronal specification in the spinal cord: inductive signals and transcriptional codes. *Nat Rev Genet* 1, 20-29.

Jung, I., Sohn, D.H., Choi, J., Kim, J.M., Jeon, S., Seol, J.H., and Seong, R.H. (2012). SRG3/mBAF155 stabilizes the SWI/SNF-like BAF complex by blocking CHFR mediated ubiquitination and degradation of its major components. *Biochem Biophys Res Commun* 418, 512-517.

Karamboulas, K., Dranse, H.J., and Underhill, T.M. (2010). Regulation of BMP-dependent chondrogenesis in early limb mesenchyme by TGFbeta signals. *J Cell Sci* 123, 2068-2076.

Khavari, P.A., Peterson, C.L., Tamkun, J.W., Mendel, D.B., and Crabtree, G.R. (1993). BRG1 contains a conserved domain of the SWI2/SNF2 family necessary for normal mitotic growth and transcription. *Nature* 366, 170-174.

Khokha, M.K., Hsu, D., Brunet, L.J., Dionne, M.S., and Harland, R.M. (2003). Gremlin is the BMP antagonist required for maintenance of Shh and Fgf signals during limb patterning. *Nat Genet* 34, 303-307.

Kim, J.K., Huh, S.O., Choi, H., Lee, K.S., Shin, D., Lee, C., Nam, J.S., Kim, H., Chung, H., Lee, H.W., *et al*. (2001). Srg3, a mouse homolog of yeast SWI3, is essential for early embryogenesis and involved in brain development. *Mol Cell Biol* 21, 7787-7795.

Kinzler, K.W., Ruppert, J.M., Bigner, S.H., and Vogelstein, B. (1988). The GLI gene is a member of the Kruppel family of zinc finger proteins. *Nature* 332, 371-374.

Kinzler, K.W., and Vogelstein, B. (1990). The GLI gene encodes a nuclear protein which binds specific sequences in the human genome. *Mol Cell Biol* 10, 634-642.

Klochendler-Yeivin, A., Fiette, L., Barra, J., Muchardt, C., Babinet, C., and Yaniv, M. (2000). The murine SNF5/INI1 chromatin remodeling factor is essential for embryonic development and tumor suppression. *EMBO Rep* 1, 500-506.

Kouzarides, T. (2007). Chromatin modifications and their function. *Cell* 128, 693-705.

Kozhemyakina, E., Ionescu, A., and Lassar, A.B. (2014). GATA6 is a crucial regulator of Shh in the limb bud. *PLoS Genet* 10, e1004072.

Lange, M., Kaynak, B., Forster, U.B., Tonjes, M., Fischer, J.J., Grimm, C., Schlesinger, J., Just, S., Dunkel, I., Krueger, T., *et al*. (2008). Regulation of muscle development by DPF3, a novel histone acetylation and methylation reader of the BAF chromatin remodeling complex. *Genes Dev* 22, 2370-2384.

Laufer, E., Nelson, C.E., Johnson, R.L., Morgan, B.A., and Tabin, C. (1994). Sonic hedgehog and Fgf-4 act through a signaling cascade and feedback loop to integrate growth and patterning of the developing limb bud. *Cell* 79, 993-1003.

Laurent, B.C., Treitel, M.A., and Carlson, M. (1991). Functional interdependence of the yeast SNF2, SNF5, and SNF6 proteins in transcriptional activation. *Proc Natl Acad Sci* 88, 2687-2691.

Laurent, B.C., and Carlson, M. (1992). Yeast SNF2/SWI2, SNF5, and SNF6 proteins function coordinately with the gene-specific transcriptional activators GAL4 and Bicoid. *Genes Dev* 6, 1707-1715.

Laurent, B.C., Treich, I., and Carlson, M. (1993). The yeast SNF2/SWI2 protein has DNA-stimulated ATPase activity required for transcriptional activation. *Genes Dev* 7, 583-591.

Lee, E.Y., Ji, H., Ouyang, Z., Zhou, B., Ma, W., Vokes, S.A., McMahon, A.P., Wong, W.H., and Scott, M.P. (2010). Hedgehog pathway-regulated gene networks in cerebellum development and tumorigenesis. *Proc Natl Acad Sci* 107, 9736-9741.

Lessard, J., Wu, J.I., Ranish, J.A., Wan, M., Winslow, M.M., Staahl, B.T., Wu, H., Aebersold, R., Graef, I.A., and Crabtree, G.R. (2007). An essential switch in subunit composition of a chromatin remodeling complex during neural development. *Neuron* 55, 201-215.

Lettice, L.A., Heaney, S.J., Purdie, L.A., Li, L., de Beer, P., Oostra, B.A., Goode, D., Elgar, G., Hill, R.E., and de Graaff, E. (2003). A long-range Shh enhancer regulates expression in the developing limb and fin and is associated with preaxial polydactyly. *Hum Mol Genet* 12, 1725-1735.

Lettice, L.A., Williamson, I., Wiltshire, J.H., Peluso, S., Devenney, P.S., Hill, A.E., Essafi, A., Hagman, J., Mort, R., Grimes, G., *et al*. (2012). Opposing functions of the ETS factor family define Shh spatial expression in limb buds and underlie polydactyly. *Dev Cell* 22, 459-467.

Li, B., Carey, M., and Workman, J.L. (2007). The role of chromatin during transcription. *Cell* 128, 707-719.

Li, D., Sakuma, R., Vakili, N.A., Mo, R., Puviindran, V., Deimling, S., Zhang, X., Hopyan, S., and Hui, C.C. (2014a). Formation of proximal and anterior limb skeleton requires early function of Irx3 and Irx5 and is negatively regulated by Shh signaling. *Dev Cell* 29, 233-240.

Li, Q., Lewandowski, J.P., Powell, M.B., Norrie, J.L., Cho, S.H., and Vokes, S.A. (2014b). A Gli silencer is required for robust repression of gremlin in the vertebrate limb bud. *Development* 141, 1906-1914.

Lickert, H., Takeuchi, J.K., Von Both, I., Walls, J.R., McAuliffe, F., Adamson, S.L., Henkelman, R.M., Wrana, J.L., Rossant, J., and Bruneau, B.G. (2004). Baf60c is essential for function of BAF chromatin remodelling complexes in heart development. *Nature* 432, 107-112.

Litingtung, Y., Dahn, R.D., Li, Y., Fallon, J.F., and Chiang, C. (2002). Shh and Gli3 are dispensable for limb skeleton formation but regulate digit number and identity. *Nature* 418, 979-983.

Logan, M., Martin, J.F., Nagy, A., Lobe, C., Olson, E.N., and Tabin, C.J. (2002). Expression of Cre Recombinase in the developing mouse limb bud driven by a Prxl enhancer. *Genesis* 33, 77-80.

Lopez-Rios, J., Speziale, D., Robay, D., Scotti, M., Osterwalder, M., Nusspaumer, G., Galli, A., Hollander, G.A., Kmita, M., and Zeller, R. (2012). GLI3 constrains digit number by controlling both progenitor proliferation and BMP-dependent exit to chondrogenesis. *Dev Cell* 22, 837-848.

Lopez-Rios, J., Duchesne, A., Speziale, D., Andrey, G., Peterson, K.A., Germann, P., Unal, E., Liu, J., Floriot, S., Barbey, S., *et al*. (2014). Attenuated sensing of SHH by Ptch1 underlies evolution of bovine limbs. *Nature* 511, 46-51.

Lu, P., Yu, Y., Perdue, Y., and Werb, Z. (2008). The apical ectodermal ridge is a timer for generating distal limb progenitors. *Development* 135, 1395-1405.

Maatouk, D.M., Choi, K.S., Bouldin, C.M., and Harfe, B.D. (2009). In the limb AER Bmp2 and Bmp4 are required for dorsal-ventral patterning and interdigital cell death but not limb outgrowth. *Dev Biol* 327, 516-523.

Mao, J., McGlinn, E., Huang, P., Tabin, C.J., and McMahon, A.P. (2009). Fgf-dependent Etv4/5 activity is required for posterior restriction of Sonic Hedgehog and promoting outgrowth of the vertebrate limb. *Dev Cell* 16, 600-606.

Mariani, F.V., Ahn, C.P., and Martin, G.R. (2008). Genetic evidence that FGFs have an instructive role in limb proximal-distal patterning. *Nature* 453, 401-405.

Michos, O., Panman, L., Vintersten, K., Beier, K., Zeller, R., and Zuniga, A. (2004). Gremlin-mediated BMP antagonism induces the epithelial-mesenchymal feedback signaling controlling metanephric kidney and limb organogenesis. *Development* 131, 3401-3410.

Muchardt, C., and Yaniv, M. (1993). A human homologue of Saccharomyces cerevisiae SNF2/SWI2 and Drosophila brm genes potentiates transcriptional activation by the glucocorticoid receptor. *EMBO J* 12, 4279-4290.

Narlikar, G.J., Fan, H.Y., and Kingston, R.E. (2002). Cooperation between complexes that regulate chromatin structure and transcription. *Cell* 108, 475-487.

Nissim, S., Hasso, S.M., Fallon, J.F., and Tabin, C.J. (2006). Regulation of Gremlin expression in the posterior limb bud. *Dev Biol* 299, 12-21.

Niswander, L., Jeffrey, S., Martin, G.R., and Tickle, C. (1994). A positive feedback loop coordinates growth and patterning in the vertebrate limb. *Nature* 371, 609-612.

Norrie, J.L., Lewandowski, J.P., Bouldin, C.M., Amarnath, S., Li, Q., Vokes, M.S., Ehrlich, L.I., Harfe, B.D., and Vokes, S.A. (2014). Dynamics of BMP signaling in limb bud mesenchyme and polydactyly. *Dev Biol* 393, 270-281.

Nusslein-Volhard, C., and Wieschaus, E. (1980). Mutations affecting segment number and polarity in Drosophila. *Nature* 287, 795-801.

Oh, J., Sohn, D.H., Ko, M., Chung, H., Jeon, S.H., and Seong, R.H. (2008). BAF60a interacts with p53 to recruit the SWI/SNF complex. *J Biol Chem* 283, 11924-11934.

Orenic, T.V., Slusarski, D.C., Kroll, K.L., and Holmgren, R.A. (1990). Cloning and characterization of the segment polarity gene cubitus interruptus Dominant of Drosophila. *Genes Dev* 4, 1053-1067.

Osterwalder, M., Speziale, D., Shoukry, M., Mohan, R., Ivanek, R., Kohler, M., Beisel, C., Wen, X., Scales, S.J., Christoffels, V.M., *et al*. (2014). HAND2 targets define a network of transcriptional regulators that compartmentalize the early limb bud mesenchyme. *Dev Cell* 31, 345-357.

Pajni-Underwood, S., Wilson, C.P., Elder, C., Mishina, Y., and Lewandoski, M. (2007). BMP signals control limb bud interdigital programmed cell death by regulating FGF signaling. *Development* 134, 2359-2368.

Pan, Y., Bai, C.B., Joyner, A.L., and Wang, B. (2006). Sonic hedgehog signaling regulates Gli2 transcriptional activity by suppressing its processing and degradation. *Mol Cell Biol* 26, 3365-3377.

Panman, L., Galli, A., Lagarde, N., Michos, O., Soete, G., Zuniga, A., and Zeller, R. (2006). Differential regulation of gene expression in the digit forming area of the mouse limb bud by SHH and gremlin 1/FGF-mediated epithelial-mesenchymal signalling. *Development* 133, 3419-3428.

Papoulas, O., Beek, S.J., Moseley, S.L., McCallum, C.M., Sarte, M., Shearn, A., and Tamkun, J.W. (1998). The Drosophila trithorax group proteins BRM, ASH1 and ASH2 are subunits of distinct protein complexes. *Development* 125, 3955-3966.

Park, H.L., Bai, C., Platt, K.A., Matise, M.P., Beeghly, A., Hui, C.C., Nakashima, M., and Joyner, A.L. (2000). Mouse Gli1 mutants are viable but have defects in SHH signaling in combination with a Gli2 mutation. *Development* 127, 1593-1605.

Phelan, M.L., Sif, S., Narlikar, G.J., and Kingston, R.E. (1999). Reconstitution of a core chromatin remodeling complex from SWI/SNF subunits. *Mol Cell* 3, 247-253.

Piette, D., Hendrickx, M., Willems, E., Kemp, C.R., and Leyns, L. (2008). An optimized procedure for whole-mount in situ hybridization on mouse embryos and embryoid bodies. *Nat Protoc* 3, 1194-1201.

Qu, S., Tucker, S.C., Ehrlich, J.S., Levorse, J.M., Flaherty, L.A., Wisdom, R., and Vogt, T.F. (1998). Mutations in mouse Aristaless-like4 cause Strong's luxoid polydactyly. *Development* 125, 2711-2721.

Riddle, R.D., Johnson, R.L., Laufer, E., and Tabin, C. (1993). Sonic hedgehog mediates the polarizing activity of the ZPA. *Cell* 75, 1401-1416.

Sanz-Ezquerro, J.J., and Tickle, C. (2000). Autoregulation of Shh expression and Shh induction of cell death suggest a mechanism for modulating polarising activity during chick limb development. *Development* 127, 4811-4823.

Sanz-Ezquerro, J.J., and Tickle, C. (2003). Fgf signaling controls the number of phalanges and tip formation in developing digits. *Curr Biol* 13, 1830-1836.

Scherz, P.J., Harfe, B.D., McMahon, A.P., and Tabin, C.J. (2004). The limb bud Shh-Fgf feedback loop is terminated by expansion of former ZPA cells. *Science* 305, 396-399.

Scherz, P.J., McGlinn, E., Nissim, S., and Tabin, C.J. (2007). Extended exposure to Sonic hedgehog is required for patterning the posterior digits of the vertebrate limb. *Dev Biol* 308, 343-354.

Selever, J., Liu, W., Lu, M.F., Behringer, R.R., and Martin, J.F. (2004). Bmp4 in limb bud mesoderm regulates digit pattern by controlling AER development. *Dev Biol* 276, 268-279.

Smith, C.L., Horowitz-Scherer, R., Flanagan, J.F., Woodcock, C.L., and Peterson, C.L. (2003). Structural analysis of the yeast SWI/SNF chromatin remodeling complex. *Nat Struct Biol* 10, 141-145.

Sohn, D.H., Lee, K.Y., Lee, C., Oh, J., Chung, H., Jeon, S.H., and Seong, R.H. (2007). SRG3 interacts directly with the major components of the SWI/SNF chromatin remodeling complex and protects them from proteasomal degradation. *J Biol Chem* 282, 10614-10624.

Sun, X., Lewandoski, M., Meyers, E.N., Liu, Y.H., Maxson, R.E., Jr., and Martin, G.R. (2000). Conditional inactivation of Fgf4 reveals complexity of signalling during limb bud development. *Nat Genet* 25, 83-86.

Sun, X., Mariani, F.V., and Martin, G.R. (2002). Functions of FGF signalling from the apical ectodermal ridge in limb development. *Nature* 418, 501-508.

Suzuki, T., Hasso, S.M., and Fallon, J.F. (2008). Unique SMAD1/5/8 activity at the phalanx-forming region determines digit identity. *Proc Natl Acad Sci* 105, 4185-4190.

Takeuchi, J.K., and Bruneau, B.G. (2009). Directed transdifferentiation of mouse mesoderm to heart tissue by defined factors. *Nature* 459, 708-711.

Tamkun, J.W., Deuring, R., Scott, M.P., Kissinger, M., Pattatucci, A.M., Kaufman, T.C., and Kennison, J.A. (1992). brahma: a regulator of Drosophila homeotic genes structurally related to the yeast transcriptional activator SNF2/SWI2. *Cell* 68, 561-572.

Tarchini, B., Duboule, D., and Kmita, M. (2006). Regulatory constraints in the evolution of the tetrapod limb anterior-posterior polarity. *Nature* 443, 985-988.

te Welscher, P., Fernandez-Teran, M., Ros, M.A., and Zeller, R. (2002a). Mutual genetic antagonism involving GLI3 and dHAND prepatterns the vertebrate limb bud mesenchyme prior to SHH signaling. *Genes Dev* 16, 421-426.

te Welscher, P., Zuniga, A., Kuijper, S., Drenth, T., Goedemans, H.J., Meijlink, F., and Zeller, R. (2002b). Progression of vertebrate limb development through SHH-mediated counteraction of GLI3. *Science* 298, 827-830.

Verheyden, J.M., and Sun, X. (2008). An Fgf/Gremlin inhibitory feedback loop triggers termination of limb bud outgrowth. *Nature* 454, 638-641.

Vokes, S.A., Ji, H., McCuine, S., Tenzen, T., Giles, S., Zhong, S., Longabaugh, W.J., Davidson, E.H., Wong, W.H., and McMahon, A.P. (2007). Genomic characterization of Gli-activator targets in sonic hedgehog-mediated neural patterning. *Development* 134, 1977-1989.

Vokes, S.A., Ji, H., Wong, W.H., and McMahon, A.P. (2008). A genome-scale analysis of the cis-regulatory circuitry underlying sonic hedgehog-mediated patterning of the mammalian limb. *Genes Dev* 22, 2651-2663.

Wang, B., Fallon, J.F., and Beachy, P.A. (2000). Hedgehog-regulated processing of Gli3 produces an anterior/posterior repressor gradient in the developing vertebrate limb. *Cell* 100, 423-434.

Wang, C., Ruther, U., and Wang, B. (2007). The Shh-independent activator function of the full-length Gli3 protein and its role in vertebrate limb digit patterning. *Dev Biol* 305, 460-469.

Wang, W., Cote, J., Xue, Y., Zhou, S., Khavari, P.A., Biggar, S.R., Muchardt, C., Kalpana, G.V., Goff, S.P., Yaniv, M., *et al*. (1996). Purification and biochemical heterogeneity of the mammalian SWI-SNF complex. *EMBO J* 15, 5370-5382.

Wang, Z., Zhai, W., Richardson, J.A., Olson, E.N., Meneses, J.J., Firpo, M.T., Kang, C., Skarnes, W.C., and Tjian, R. (2004). Polybromo protein BAF180 functions in mammalian cardiac chamber maturation. *Genes Dev* 18, 3106-3116.

Witte, F., Chan, D., Economides, A.N., Mundlos, S., and Stricker, S. (2010). Receptor tyrosine kinase-like orphan receptor 2 (ROR2) and Indian hedgehog regulate digit outgrowth mediated by the phalanx-forming region. *Proc Natl Acad Sci* 107, 14211-14216.

Wong, Y.L., Behringer, R.R., and Kwan, K.M. (2012). Smad1/Smad5 signaling in limb ectoderm functions redundantly and is required for interdigital programmed cell death. *Dev Biol* 363, 247-257.

Wu, J.I., Lessard, J., Olave, I.A., Qiu, Z., Ghosh, A., Graef, I.A., and Crabtree, G.R. (2007). Regulation of dendritic development by neuron-specific chromatin remodeling complexes. *Neuron* 56, 94-108.

Xu, B., Hrycaj, S.M., McIntyre, D.C., Baker, N.C., Takeuchi, J.K., Jeannotte, L., Gaber, Z.B., Novitch, B.G., and Wellik, D.M. (2013). Hox5 interacts with Plzf to restrict Shh expression in the developing forelimb. *Proc Natl Acad Sci* 110, 19438-19443.

Zeller, R., Lopez-Rios, J., and Zuniga, A. (2009). Vertebrate limb bud development: moving towards integrative analysis of organogenesis. *Nat Rev Genet* 10, 845-858.

Zhan, X., Shi, X., Zhang, Z., Chen, Y., and Wu, J.I. (2011). Dual role of Brg chromatin remodeling factor in Sonic hedgehog signaling during neural development. *Proc Natl Acad Sci* 108, 12758-12763.

Zhang, Z., Verheyden, J.M., Hassell, J.A., and Sun, X. (2009). FGF-regulated Etv genes are essential for repressing Shh expression in mouse limb buds. *Dev Cell* 16, 607-613.

Zhang, Z., Sui, P., Dong, A., Hassell, J., Cserjesi, P., Chen, Y.T., Behringer, R.R., and Sun, X. (2010). Preaxial polydactyly: interactions among ETV, TWIST1 and HAND2 control anterior-posterior patterning of the limb. *Development* 137, 3417-3426.

Zhu, J., Nakamura, E., Nguyen, M.T., Bao, X., Akiyama, H., and Mackem, S. (2008). Uncoupling Sonic hedgehog control of pattern and expansion of the developing limb bud. *Dev Cell* 14, 624-632.

Zhulyn, O., Li, D., Deimling, S., Vakili, N.A., Mo, R., Puviindran, V., Chen, M.H., Chuang, P.T., Hopyan, S., and Hui, C.C. (2014). A switch from low to high Shh activity regulates establishment of limb progenitors and signaling centers. *Dev Cell* 29, 241-249.

Zuniga, A., Haramis, A.P., McMahon, A.P., and Zeller, R. (1999). Signal relay by BMP antagonism controls the SHH/FGF4 feedback loop in vertebrate limb buds. *Nature* 401, 598-602.

Zuniga, A., Laurent, F., Lopez-Rios, J., Klasen, C., Matt, N., and Zeller, R. (2012). Conserved cis-regulatory regions in a large genomic landscape control SHH and BMP-regulated Gremlin1 expression in mouse limb buds. *BMC Dev Biol* 12, 23.

국문 초록

발생과 분화 중에 유전자 발현의 변화는 염색사 상태의 변형을 필요로 하는데, 이는 전사인자가 유전자 조절요소로의 접근을 허용하거나 제한한다. 발생이 진행되면서, 발생 신호에 반응하는 조직특이적인 전사인자들은 염색사 리모델링 단백질들을 유전자 조절요소로 불러들인다. 최근 연구들은 조직의 패턴화를 이해하는데 유용한 연구모델인 사지싹을 이용해 유전체 내에서 이러한 인자들의 상호연결된 전사적 네트워크를 구축해왔다. 따라서 사지발생을 통제하는 조절자들의 분자회로는 염색사 리모델링 단백질들의 구분되는 기능을 수반한다. 점이화된 Sonic hedgehog (Shh) 신호전달은 활성인자 혹은 억제인자로 작용하는 두 기능을 함께 가지는 Gli 전사인자들의 활성을 조절하여 전후축을 따라 사지골격을 패턴화하는데 지배적으로 기능한다. Gli 표적유전자들은 점이화된 Hedgehog (Hh) 신호전달에 반응하여 활성화, 억제화, 혹은 탈억제화되지만 Gli 단백질들이 표적유전자들을 조절하기 위하여 작용하는 기작은 이해가 부족하다. 또한 사지 패턴화에 관여하는 유전적 네트워크는 잘 정의되어 있지만 염색사 리모델링 단백질들에 의한 후성적 조절 과정은 잘 알려져 있지 않다.

본 연구에서 나는 SWI/SNF 염색사 리모델링 복합체의 핵심 요소인 Srg3/mBaf155 가 Shh/Gli 에 의한 사지 전후골격 패턴화에 필수적인 기능을 한다는 것을 관찰하였다. 유전학적 분석과 whole-mount in situ hybridization 실험기법을 통해 분석된 유전자 발현의 시공간적 분포는 사지발생 중의 Hh 경로에서 SWI/SNF 복합체의 두 가지 필요성을 보여주었다. 사지짝에서 간엽

특이적인 Srg3 의 제거는 Shh 자극 중에 Shh 의 수용기 Ptch1 과 하위 작동인자 Gli1 의 유전자 발현의 증가를 저해하였고, Shh 이 없는 영역에서 비정상적으로 Hh 경로의 유전자 발현을 활성화하였다. 또한 Srg3 가 결핍된 사지싹에서 Shh 감지의 감소는 표적유전자 발현의 감소뿐만 아니라 Shh 후손 세포들의 재배열로 이어졌다. Srg3 결핍 사지싹은 신호발생 중추인 zone of polarizing activity (ZPA)와 apical ectodermal ridge (AER)의 형성이 정상적으로 일어나고 온전한 전후축이 확립되지만, 점진적으로 전후 정체성을 상실한다. 이러한 점진적 표현형의 분석은 Shh 반응성의 조절이 후측 사지골격 전구세포의 운명을 조정하고 비정상적 Hh 경로의 활성화가 전측 골격 형성에 해롭게 작용한다는 유전적 증거를 제공한다. Hh 경로에서 Srg3 결핍은 Shh, Bmp 대립자 Gremlin1 (Grem1), Fgf 와 같은 상피-배엽간 신호전달의 분포를 말단화하고, 이어서 zeugopod 과 autopod 의 원시세포에서 Bmp 활성에 문제를 야기하고 연골분화를 붕괴시킨다. 특히 나는 Shh 반응성과 Gli 억제인자의 활성도가 발가락 연골형성의 시작에 영향을 끼치는 Grem1 의 시공간적 발현을 협력적으로 조절함을 관찰하였다. 본 연구는 사지골격 전구세포의 운명을 결정하는 Hh 경로에서 SWI/SNF 복합체의 기능을 보여준다.

주요어: SWI/SNF, Srg3, 사지발생, Hedgehog (Hh), Grem1

학번: 2007-30094